Effects of basalt, concrete fines, and steel slag on maize growth and toxic trace element accumulation in an enhanced weathering experiment

Jet Rijnders[1*], Arthur Vienne[1], Sara Vicca[1]

[1]*Biobased Sustainability Engineering (SUSTAIN), Department of Bioscience Engineering, University of Antwerp, Groenenborgerlaan 171, 2020 Antwerpen, Belgium*

**Correspondence to*: Jet Rijnders (jet.rijnders@uantwerpen.be)

Abstract.

Terrestrial enhanced silicate weathering is a CO_2 removal technology involving the application of ground silicate materials to agricultural soils. Next to CO_2 sequestration, it can improve soil fertility and crop growth, but silicate materials can also contain toxic trace elements. In a mesocosm experiment, we investigated the effect of basalt, concrete fines and steel slags on biomass, nutrients, and toxic trace element concentration of Zea Mays, using a dose-response approach.

Plant biomass increased with basalt, but not with concrete fines and steel slags. Generally, plant Ca, Mg, and corn Si concentrations increased with increasing silicate application amount as a result of increased plant availability. In contrast, plant N, P, and K concentrations were hardly affected by silicate application. Besides increased leaf Pb concentrations with steel slag application, which did not exceed the maximum limit set by the WHO and FAO (0.05 mg Pb kg^{-1} ww), toxic trace element concentrations in aerial plant tissues mostly decreased with increasing silicate application amount, presumably because of an increased soil pH, and accumulation in plant roots. Our study thus indicates mixed effects of silicate application on maize while suggesting that the risk of toxic trace element contamination after a one-time application of the tested silicates is limited.

1. Introduction

Recently, there has been a growing interest in the use of silicate rock powder in agriculture for carbon dioxide (CO_2) removal (Edwards et al., 2017; Swoboda et al., 2022). When silicates react with water and CO_2, (bi)carbonates are formed that can be transported to the ocean via leaching into the ground water, possibly storing carbon (C) for centuries and longer (Moosdorf et al., 2014). While the naturally occurring silicate rock weathering process has been important for stabilizing climate at geological timescales, its pace is insufficient to substantially reduce the current rise in atmospheric CO_2 (Berner, 2004; Walker et al., 1981). Enhanced silicate weathering (EW) aims to accelerate this natural process through the mechanical grinding of the rocks into a fine powder.

In addition to its atmospheric CO_2 removal potential, applying silicate minerals to soils holds promise for improving agricultural practices. When silicate minerals weather, protons are consumed and weathering products, such as calcium (Ca^{2+}) and magnesium (Mg^{2+}), are released (Kelland et al., 2020; Ramos et al., 2022). This can improve soil chemical properties such as increasing soil pH and cation exchange capacity (CEC), and improvement of soil water retention (Anda et al., 2015; Calabrese et al., 2022; Taylor et al., 2017). Soil acidification and nutrient leaching are pervasive issues in agriculture, and EW can in this way contribute to soil health and improve crop growth (Tilman et al., 2002). Additionally, even though not considered an essential plant nutrient, the process of EW releases silicon (Si), which can improve plant resistance to pests and diseases, thereby improving crop health and productivity in general (Calabrese et al., 2022; Swoboda et al., 2022). Because of these benefits, silicate rock powder has been used as a fertilizer for many years (Van Straaten, 2006), particularly in tropical regions, where the release of base cations from these rocks can significantly enhance crop productivity (e.g. Swoboda et al., 2022). Nonetheless, EW also holds certain risks that need to be considered. Silicate materials typically contain toxic trace elements that are released into the environment during weathering, posing the risk of uptake by plants. The amount of toxic trace elements varies strongly among rocks and industrial silicates (Dupla et al., 2023; O'Connor et al., 2021). For instance, basalt, a naturally occurring and globally abundant silicate rock, generally exhibits lower concentrations of potentially harmful metals such as nickel (Ni) and chromium (Cr) compared to other silicate rock types and is therefore a preferred rock source to consider in agriculture (Kelland et al., 2020). Basalt is a mafic igneous rock that contains substantial amounts of Ca- and Mg-rich silicate minerals (Lewis et al., 2021). In the review of Swoboda et al. (2022), all trials with (ultra)mafic rocks on agricultural soils improved yields. Recent studies further corroborate these findings; Luchese et al. (2023), for instance, documented improved corn biomass upon basalt application in both clay and sandy clay loam soils. Similarly, basalt addition led to notable increases in dry mass, height and stem diameter, and the accumulation of macronutrients (Nitrogen (N), Phosphorous (P), potassium (K), Sulphur (S), Ca and Mg) in corn and beans grown on tropical soils (Conceição et al., 2022).

Most EW experiments have been conducted in tropical regions on highly weathered, acidic soils, while studies in a temperate climate are still scarce (Swoboda et al., 2022). Yet, Skov et al. (2024) demonstrated an increase in spring oat yield after application of basalt on direct drill and ploughed plots in a temperate climate. These increases were assigned to a modest increase in pH that resulted in reduced manganese (Mn) and iron (Fe) uptake. This study also reported higher tissue Ca content and increased grain and tissue K upon basalt application. Contrastingly, the addition of volcanic rock dust to soils did not influence wheat growth in a mesocosm experiment in Sweden (Ramezanian et al., 2013). Furthermore, the aboveground biomass of potato plants tended to increase with basalt application in a mesocosm experiment in Belgium, growing on an alkaline soil (Vienne et al., 2022). Nonetheless, it is important to keep in mind that the apparent dominance of positive EW effects on crop growth might be affected by publication bias, as negative or non-significant results are less likely to be published compared to positive and expected outcomes (Dieleman & Janssens, 2011).

While the use of geological silicates requires energy for the mining and grinding of rocks, thereby partially offsetting the CO_2 removal potential (Beerling et al., 2020; Goll et al., 2021), this energy cost may be strongly reduced by using silicate materials derived from industrial processes. For instance, Ca-rich silicates generated as by-products from steel manufacturing (steel slag) or waste concrete fines, represent alternatives that circumvent the need for additional mining (Renforth et al., 2011). These industrial by-products contain minerals that dissolve faster than basalt and are already produced in fine particle sizes, thereby diminishing the energy cost of grinding (Beerling et al., 2020).

Concrete waste has previously been applied to soils to improve plant growth but how it affects plants is currently poorly understood (Ho et al., 2021). Concrete by-products are produced in large quantities because concrete is a popular product throughout the construction industry (dos Reis et al., 2020). Concrete fines also contain silicate minerals, and other cations, such as Fe, Ca, and Mg (Table 2), but almost 18% of the concrete fines used in this study is calcite ($CaCO_3$) (Table S1). Calcite dissolution does not lead to net uptake of CO_2, because all CO_2 that is consumed during dissolution is returned back to the atmosphere by precipitation of carbonates in the ocean (Liu et al., 2011). Therefore, weathering of concrete fines will probably be less efficient for carbon capture. In contrast, the application of steel slag as a fertilizer in agriculture is already a common practice (Gao et al., 2020). Various trials demonstrated increases in biomass upon steel slag application, for instance for soybean (Castro & Crusciol, 2013; Deus et al., 2020), maize (Castro & Crusciol, 2013; Wang & Qing-sheng, 2006) and rice (Makabe-sasaki & Sasaki, 2015; Wang et al., 2015). At three different locations in Germany, long-term field trials with steel slag application have been running since 1954, 1990 and 1993. At all locations, the yield of grass or arable crops increased significantly with the application of different kinds of steel slags, despite increases in Cr and Vanadium (V) contents in the soil (Branca et al., 2014). Nonetheless, as with other silicate materials, research about its influence on crops in temperate climates is lacking, and the fate of potential toxic elements is unknown.

Despite the evident benefits, there remain substantial gaps in our understanding of the broader implications of EW in agriculture. Specifically, its influence on nutrient cycling and the potential for contamination with toxic trace elements, particularly with industrial by-products such as concrete fines and steel slag, warrants further investigation. Most research so far has been conducted in a tropical climate (Swoboda et al., 2022), often on highly weathered and acidic soils, but EW is currently considered for application also in other climate regions and thus a better understanding is needed.

This study aims to quantify the influence of basalt, concrete fines, and steel slag on *Zea mays* growth, yield, and nutrient and toxic trace element concentrations in a mesocosm experiment in a temperate climate. The three types of silicates were applied in a dose-response approach ranging from 0 to 200 ton ha^{-1} of basalt, 0 to 31 ton ha^{-1} of concrete fines, and 0 to 10 ton ha^{-1} of steel slag. We hypothesized that: I) Availability of weathering products increase with increasing silicate application amount; II) Plant biomass and plant concentrations of nutrients present in the silicates increase with increasing silicate application, and III) toxic trace elementconcentrations increase with increasing silicate application, especially with basalt and steel slag, as they contain Cr, Ni and V, and Cr and V respectively, while these are absent in the concrete fines.

2. Materials and methods

2.1 Experimental set-up

Thirty mesocosms (0.6 m height, radius = 0.25 m) were constructed at the experimental site at the Drie Eiken Campus of the University of Antwerp, Belgium (51º09' N, 04º24' E) , and placed outdoors to receive natural rainfall (Fig. 1a). In May 2021, the bottom 40 cm of each mesocosm was filled with a sandy-loam soil obtained from a pasture in Zandhoven, Belgium (Table 1). The upper 20 cm was filled with the same soil, either unamended in the control treatment (5 replicates), or amended with one of three different types of silicates (basalt, concrete fines, or steel slag) mixed into the topsoil layer on May 10, 2021.

Table 1: Soil characteristics of the original soil, before the start of the experiment.

Texture (Sand, clay, silt %)	Sandy loam (61, 4, 35)
pH	5.94 ± 0.03
Organic C (%)	0.234 ± 0.005
Inorganic C (%)	0.024 ± 0.018
Cation exchange capacity (meq $100g^{-1}$)	2.5

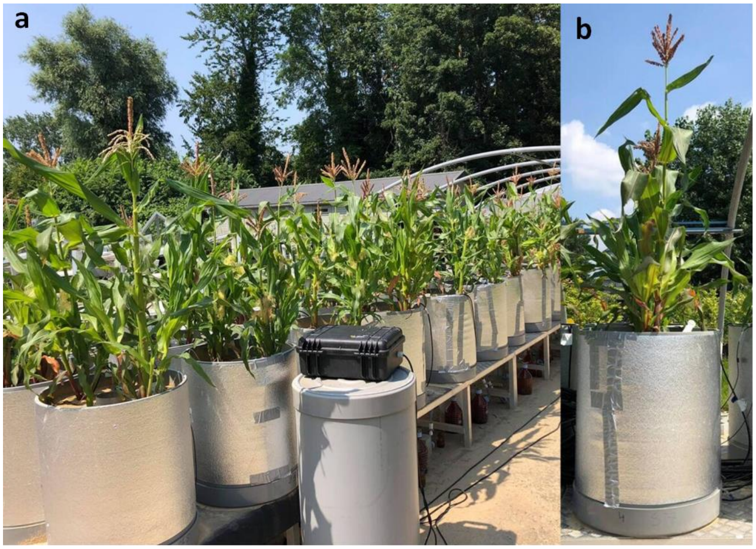

Figure 1: a) overview of the experiment; b) one mesocosm with two maize plants.

Table 2: Elemental composition (C=concentration) of basalt, concrete fines and steel slags.

Basalt		Concrete fines		Steel slags	
Element	**C (wt%)**	**Element**	**C (wt%)**	**Element**	**C (wt%)**
Si	14.70%	Si	34.73%	Ca	42.00%
Fe	8.58%	Ca	9.41%	Fe	18.30%
Ca	6.42%	Fe	2.52%	Si	4.93%
Mg	5.88%	Al	2.36%	Mn	2.20%
Al	5.16%	K	1.20%	Mg	0.97%
Na	1.87%	Mg	0.63%	Al	0.90%
Ti	1.08%	Na	0.41%	P	0.77%
K	0.77%	S	0.27%	Ti	0.47%
P	0.26%	Ti	0.18%	V	0.32%
Mn	0.15%	Zr	0.15%	Cl	0.28%
Cl	765 PPM			S	0.13%
Sr	739 PPM			Cr	0.12%
Ba	559 PPM			Nb	302 PPM
Ni	408 PPM			Sr	277 PPM
Cr	367 PPM			Zr	164 PPM
V	242 PPM			K	105 PPM
Ce	197 PPM			Zn	58.3 PPM
Zr	150 PPM				
Zn	103 PPM				
S	93.3 PPM				
Cu	75.2 PPM				
Nb	61.0 PPM				
Rb	24.3 PPM				
Y	20.4 PPM				
Co	3.18 PPM				

Eifel Basalt, with P80 = 310.78 µm, was obtained from DURUBAS (https://www.rpbl.de) (Table S1, S2). Blast-oxygen furnace slag (BOF-slag, hereafter referred to as steel slag), with P80 = 201.65 µm were sourced from ArcelorMittal Ghent (https://belgium.arcelormittal.com) (Table S1, S2). Concrete waste was obtained from a local concrete recycling company (RECYBO, http://www.recybo.be) and dry sieved over a 2 mm sieve (Table S1, S2). The fraction <2 mm is further referred to as 'concrete fines'. The elemental composition of the silicate materials can be found in Table 2.

A dose-response experiment was established, where the silicates were amended in different concentrations: seven application amounts of basalt (10 to 200 ton ha^{-1}), seven application amounts of concrete fines (7 to 31 ton ha^{-1}) and seven application amounts of steel slag (1 to 10 ton ha^{-1}) (Table 3). For basalt, there were five replicates of 50 ton ha^{-1} because it is commonly used in previous studies about EW (Gillman et al., 2001; Swoboda et al., 2022). The application rates were selected based on typical applications found in literature, while also aiming for similar neutralizing effects among silicate materials (based on the CaO and MgO in the materials and a small lab test with the materials) (e.g. Kelland et al., 2020; White et al., 2017). Concrete fines could weather faster than 10^{-6} mol m^{-2} s^{-1}, depending on their carbonation (Palandri & Kharaka, 2004) and the dissolution rate of steel slag ranges between 10^{-9} and 10^{-7} mol m^{-2} s^{-}

[1] (De Windt et al., 2011). This is faster compared to the weathering rates of basalt (10^{-12} – 10^{-10} mol m^{-2} s^{-1}) (Gudbrandsson et al., 2011). Therefore, the application rate of basalt covers a wider range compared to concrete fines and steel slag.

Table 3: Application rates of basalt, concrete fines and steel slag and number of replicates for each application rate. The five replicates where no silicate material was applied are the same mesocosms for the three treatments, i.e. the experiment contained five control treatments.

Basalt		**Concrete fines**		**Steel slag**	
Application amount (ton ha^{-1})	*Replicates*	*Application amount (ton ha^{-1})*	*Replicates*	*Application amount (ton ha^{-1})*	*Replicates*
0	5	0	5	0	5
10	1	7.04	1	2	1
30	1	10.57	1	3	1
50	5	14.09	1	4	1
75	1	17.62	1	5	1
100	1	21.15	1	6	1
150	1	24.67	1	7	1
200	1	31.07	1	10	1

Each mesocosm was equipped with a 2 cm diameter hole at the bottom for leachate collection, and a root exclusion mat covered the bottom of the mesocosm to prevent soil export through leaching. Glass collectors with a volume of 2.3 L were connected to the mesocosm via polyurethane tubing. On June 3, 2021, two sweet corn seedlings (variety Tom Thumb, purchased at Le Grenier) were planted in each mesocosm (Fig. 1b), and all pots were fertilized with nitrogen, phosphorous, and potassium (NPK; 96 – 10 – 79 kg ha-1) by adding $Ca(NO_3)_2$, triple super phosphate (TSP, 45% P_2O_5) and K_2SO_4. The fertilization amount was similar to that used in Ven et al. (2019), except for P, which was halved to avoid overfertilization in combination with the added silicates.

Soil water content and temperature were monitored using Cambell Scientific sensors (CS616) in each mesocosm (Fig. S2). Precipitation and air temperature for the duration of the experiment were retrieved from visualcrossing (https://www.visualcrossing.com/) (Fig. S3). Mesocosms were also watered manually (Table S2) at the beginning of the experiment and during dry periods. Analysis to determine the CO_2 removal potential in this study were performed, an in-depth assessment of the weathering rates and CO_2 removal are presented in Vienne et al (submitted).

2.2 Plant measurements

Throughout the growing season, plant height was monitored at ten times. On July 15 and August 11, 2021, leaf area index (LAI) was determined for each mesocosm, following the approach of Ven et al. (2019). For every plant, the numbers of leaves were counted (nleaf) and the width (Wleaf) and length (Lleaf) of each leaf were measured. First, individual leaf area (LA) was calculated using the conversion factor Aleaf = 0.75 for maize (Montgomery, 1911) (eq 1).

$$LA = L_{leaf} * W_{leaf} * A_{leaf} \quad \text{(eq 1)}$$

Leaf Area Index (LAI) was then calculated for each mesocosm, with A the area of the mesocosms (0.20 m²) (eq 2).

$$LAI = LA * n_{plant} * n_{leaf} * (A)^{-1} \quad \text{(eq 2)}$$

Plants were harvested on August 26, 2021, starting with the top leaf of each plant for further analysis. The aboveground biomass was then harvested and separated into stems, leaves, tassels, and corn. A week after harvesting, roots were sampled from topsoil (0-20 cm) and subsoil (20-60 cm) to estimate the root biomass within each mesocosm. One soil core (100 cm³) was taken below the shoot of each plant (thus a total of two cores per mesocosm for each soil layer, as each mesocosm contains two plants), and one core for each soil layer at the centre of the mesocosms. A similar method was used in Ven et al. (2020) where they were able to close the C balance using a similar approach, demonstrating its accuracy. Subsequently, soil was carefully rinsed over a 2 mm sieve positioned above a receptacle. Roots were collected from the sieve, including those floating on the water in the receptacle. After drying for 48h at 70 °C, the dry weight (dw) of each plant part was determined. For roots, the average dry root biomass (g cm³) was calculated assuming that the core from the centre of the mesocosm represented 50% of the root distribution across the surface area, while each of the two cores underneath the plants accounted for 25% each. Plant samples (aboveground and root biomass) were dried at 70 °C for 48h.

Leaves, stems, tassels, corn seeds, and roots were ground using a centrifugal mill (model ZM 200, Retsch GmbH, Haan, Germany) with a sieve of 0.25 mm mesh size. All ground samples were analysed for nutrients (Ca, Fe, K, Mg, P, Si) through ICP-OES (iCAP 6300 duo, Thermo Scientific) and C and N content by dry combustion, based on the Dumas method using an elemental analyser (model FLASH 2000, Interscience, Louvain-la-Neuve, Belgium). Leaves, stems, tassels and corn seeds were also analysed for toxic trace elements (cadmium (Cd), Cr, Ni, lead (Pb), V). Due to limited root samples that were harvested, toxic trace element concentrations were not analysed in our study. For each plant sample, 0.3 g was weighed and digested with H_2SO_4, salicylic acid, H_2O_2 and selenium to determine Ca, Fe, K, Mg, and P and the toxic trace elements listed above according to Walinga et al. (1995). Si was determined by digestion of 30 mg plant sample with 25 mL O.5 N NaOH. Pb and Ni concentrations were compared to the maximum allowable levels. As these are reported per g ww of plant material, we converted our concentrations from dw to ww. For corn Pb, the Limit of Quantification (LOQ) (0.1 mg kg^{-1} dw) was used since all Pb concentrations in corn were lower.

2.3 Soil measurements

Starting from May 19, 2021, soil porewater samples were collected weekly for chemical analysis using rhizons (Rhizon Flex, Rhizosphere Research Products B.V., Wageningen, NL) installed at 5 cm depth in each mesocosm. Soil porewater pH was measured with a Metrohm 914 pH/Conductometer. For chemical analysis, samples were filtered through a 0.45 µm PET filter. Concentrations of Ca, Cd, Cr, Fe, Mg, Ni, Pb, Si, and V were analysed with ICP-OES (iCAP 6300 duo, Thermo

Scientific). DIC was measured with a Skalar (Formacs ^{HT}). Ca, Fe, K, Mg and Si and DIC were analysed weekly, while Cd, Cr, Ni, Pb, and V were analysed once on August 18, 2021, near the end of the growing season.

Topsoil pH was measured on five occasions (May 25, June 10, and 24, July 19, and August 4) by collecting and pooling three subsamples per mesocosm from right underneath the soil surface ($\pm$ 1 cm). Subsequently, 4 g of soil was suspended in 10 mL of deionized water and shaken before analysis using a Metrohm 914 pH/Conductometer meter. Plant Root Simulator probes (PRS™, Western Ag Innovations, Saskatoon, Canada) were inserted into the soil twice: on June 24 and August 02, 2021. They were retrieved one week later, on July 01 and August 09, 2021, respectively. More information about these ion exchange membranes is provided by (Qian & Schoenau, 2002). Soil CEC was determined following the protocol of Brown (1943) for which approximately 2.5 g of air-dried soil was extracted with 1 M NH_4Acetate for 1h at room temperature with continuous agitation. Extracts were measured with ICP-OES (iCAP 6300 duo, Thermo Scientific).

2.4 Statistical analysis

All statistical analyses were conducted in R (Rstudio, 2021.09.0.0). The level of significance for all analyses was set at $p \leq 0.05$. Data normality of residuals was checked using the Shapiro–Wilk test and the homoscedasticity of the residuals was examined by plotting them against the fitted values. In case one of these assumptions was violated, a logarithmic, inverse or square root transformation was applied to the data. Plots were designed with the ggplot2 package(Wickham, 2016), ggpubr package (Kassambara, 2023) and the Rmisc package (Hope, 2023).

Linear regression analyses were performed to explore the relationship between the application amount of each silicate material separately and the variables of interest, i.e. plant biomass, nutrient and toxic trace element content of the different plant parts, toxic trace element content of the porewater and soil CEC. If the normality or homoscedasticity of the residuals of the linear model was not met after data transformation, a non-parametric Kruskal-Wallis test was used. To assess changes over time and differences among application amounts for each silicate type, a linear mixed model (nlme package (Pinheiro et al., 2013)) was applied for plant height, soil pH, soil porewater pH, soil porewater DIC, soil porewater nutrient concentrations, and nutrient availability from the PRS probes. Silicate application amount, time (days after sowing, or burial date for the nutrient availability from the PRS probes), and their interaction were included as fixed effects, while mesocosm was treated as a random effect. To account for heteroscedasticity in the data across different time points, the weights = varIdent component was incorporated into the model. Differences among silicates were investigated using method S1.

To investigate which soil parameters are linked with differences in biomass, a linear model was constructed based on the Akaike information criterion (AIC). All soil parameters (soil pH, CEC, porewater pH, porewater nutrients, and porewater toxic trace elements) were included in the original model, whereafter the best fit was selected with the lowest AIC score. Hereafter, a two-way ANOVA was performed to search for soil parameters that significantly influence plant biomass. To reduce the complexity of the data, a principle component analysis (PCA) was done to explore differences in soil variables (soil and porewater pH, CEC, porewater nutrients, and porewater toxic trace elements) among the three silicate treatments. Linear regression analysis was performed with each principal component (PC) as a function of silicate treatment and as a function of plant biomass.

3. Results

3.1 Soil chemistry

Application of basalt, concrete fines, and steel slag resulted in significant increases in soil pH, with the most pronounced increases for concrete fines and steel slag (Fig. 2, Table S3). Porewater pH and DIC generally increased as well with basalt, concrete fines, and steel slag application amount (Fig. 2, Table S3) with a more pronounced DIC increase with increasing steel slag application amount compared to basalt and concrete fines (Fig. 2, Table S4). The basalt effect on DIC increased over time while the steel slag effect slightly decreased as the growing season progressed (Fig. 2).

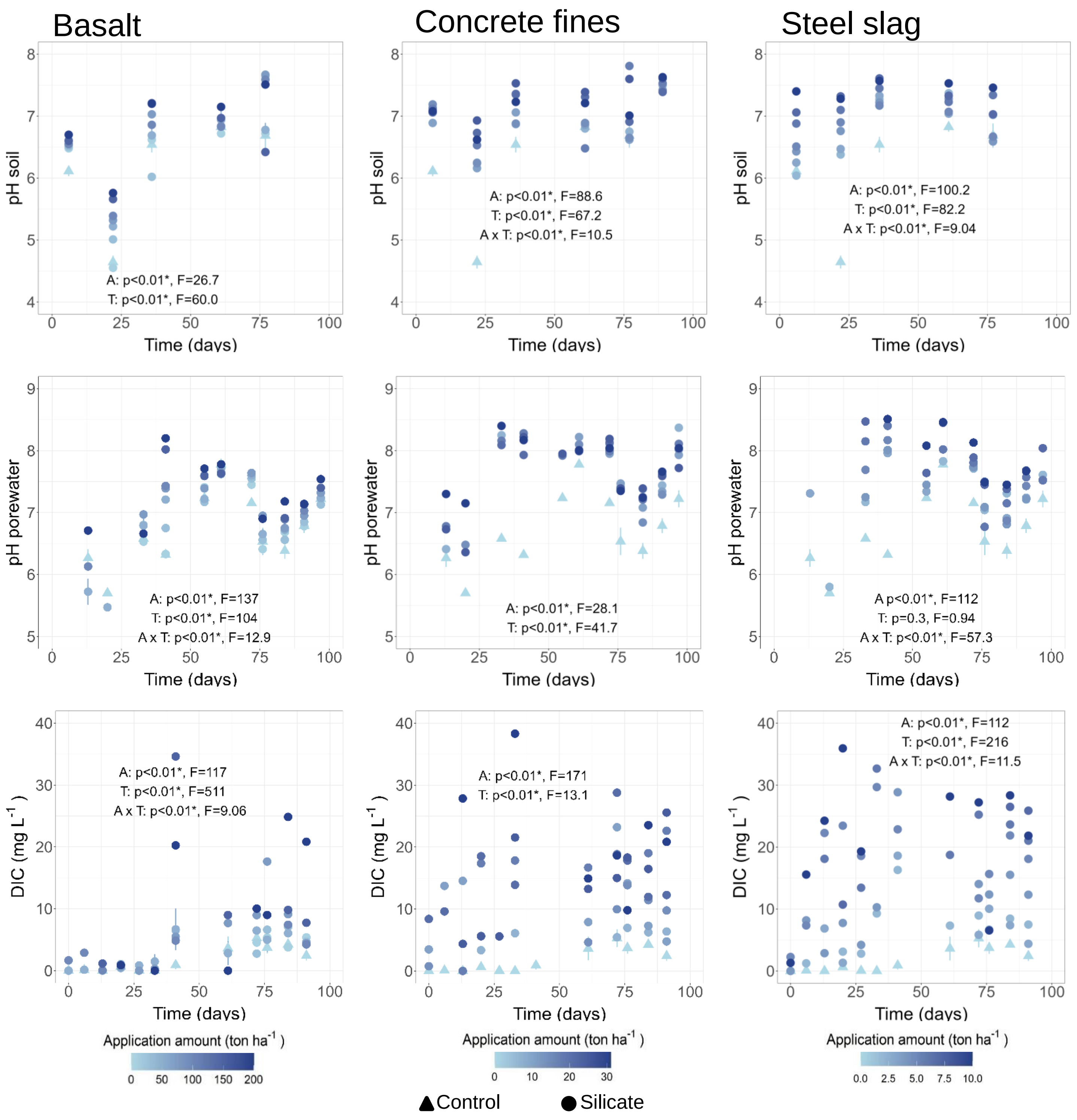

Figure 2: Soil pH, porewater DIC and porewater pH during the experiment for basalt, concrete fines and steel slag treatments. Control treatment (0 ton ha $^{-1}$) and basalt treatment with an application rate of 50 ton ha^{-1} are averages of five replicates and are shown with standard error. The other treatments each have one replicate. P-values and F-values are shown from linear regression analysis with soil pH, porewater pH or DIC as fixed effect and silicate application amount, time and the interaction as covariables. If the interaction was not statistically significant, this was deleted from the model and thus not shown here. Statistically significant relationships are indicated by an asterisk (*).

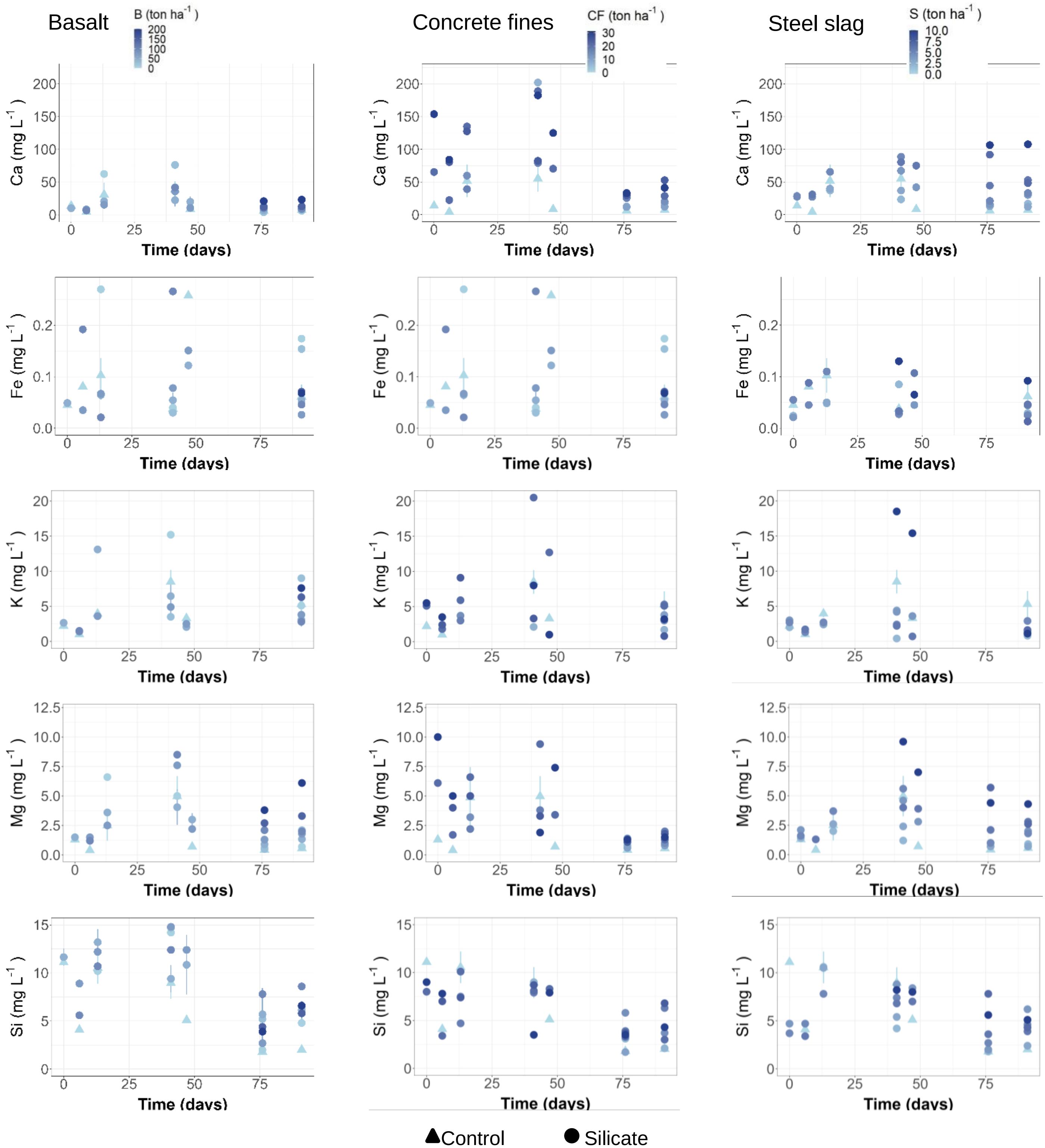

Figure 3: Ca, Fe, K, Mg and Si in the porewater during the experiment for the silicate treatments (basalt, concrete fines, steel slag). Control treatment (0 ton ha $^{-1}$) and basalt treatment with an application rate of 50 ton ha^{-1} are averages of five replicates and are shown with standard error. Note that in some cases, the error bars are smaller than the symbol. The other treatments have one measurement each. P and F-values are shown in Table S3.

The influence of silicate application on soil porewater Ca concentrations varied among silicate material types (Fig. 3, Table S4). Increases were observed with increasing application amount of concrete fines and steel slag (Fig. 3, Table S3), which is similar to plant available Ca from PRS probes (Fig. S3). Conversely, porewater Ca concentrations decreased with increasing basalt application amount. However, data for the highest application amounts of basalt (150 and 200 ton ha^{-1}) are only available for the last two sampling dates, during which Ca concentrations increased with increasing basalt application amount ($p< 0.01$, $F=26.38$, statistical analysis only performed on the last two sampling dates). This increase is supported by data retrieved from the PRS probes, where plant-available Ca increased with basalt application amount (Fig. S3). Nonetheless, plant-available Ca was lower with basalt compared to concrete fines and steel slag application (Table S5).

A significant time x application amount interaction effect was found for Mg and Si concentrations in the soil porewater (Fig. 3, Table S3). Both increased with basalt, concrete fines, and steel slag application amount, yet the positive effect on Mg concentrations diminished towards the end of the growing season (Fig. 3, Table S3). Plant available Mg from the PRS probes increased as well with basalt and concrete fines application amount (Fig. S4). Increases in Si with basalt and steel slag were higher at the beginning of the experiment, while increases in Si with concrete fines application amount were relatively constant over time (Fig. 3, Table S3). In contrast, Fe concentrations decreased with increasing concrete fines application amount whereas these were not affected by basalt or steel slag application (Fig. 3, Table S3). However, this was not supported by the bioavailability of Fe retrieved from the PRS probes, which was not affected by silicate application (Fig. S3). Porewater K concentrations significantly decreased with steel slag application amount, whereas no effects were observed with basalt and concrete fines (Fig. 3, Table S3).

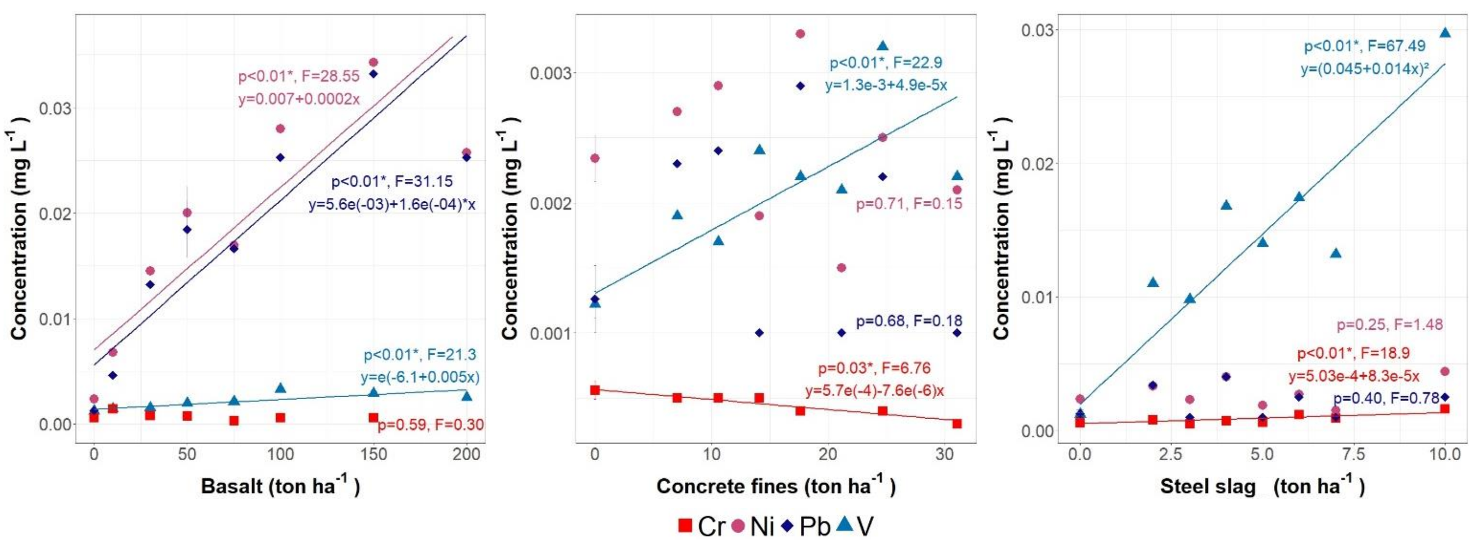

Figure 4: Concentrations of Cr, Ni, Pb and V in the porewater at the end of the growing season for basalt, concrete fines and steel slag treatments. Control treatment (0 ton ha^{-1}) and basalt treatment with an application rate of 50 ton ha^{-1} are averages of five replicates and are shown with standard error. The other treatments each have one replicate. P-values and F-values are shown from a linear regression analysis with toxic trace element (Cr, Ni, Pb, V) concentration as fixed effect and silicate application amount as covariable. Statistically significant relationships are indicated by an asterisk

In over 73% of the porewater samples, Cd concentrations were below the LOQ (Table S6), rendering statistical analysis unfeasible. Cr concentrations remained unaffected by basalt, whereas a decrease was observed with increasing application amount of concrete fines, in contrast to increasing Cr concentrations with increasing steel slag application amount (Fig. 4, Table S4). Porewater Ni and Pb concentrations increased with basalt application amount, yet remained unaffected by concrete fines or steel slag application. Moreover, these concentrations were higher with basalt compared to concrete fines and steel slag application (Fig. 4, Table S4). These changes in Pb concentrations contrast with PRS probe data, where Pb increased with concrete fines application but remained unchanged with basalt and steel slag application amount (Fig. S4, Table S5). Porewater V concentrations were higher with steel slag application compared to basalt and concrete fines and increased with application amount of basalt, concrete fines and steel slag (Fig. 4, Table S4).

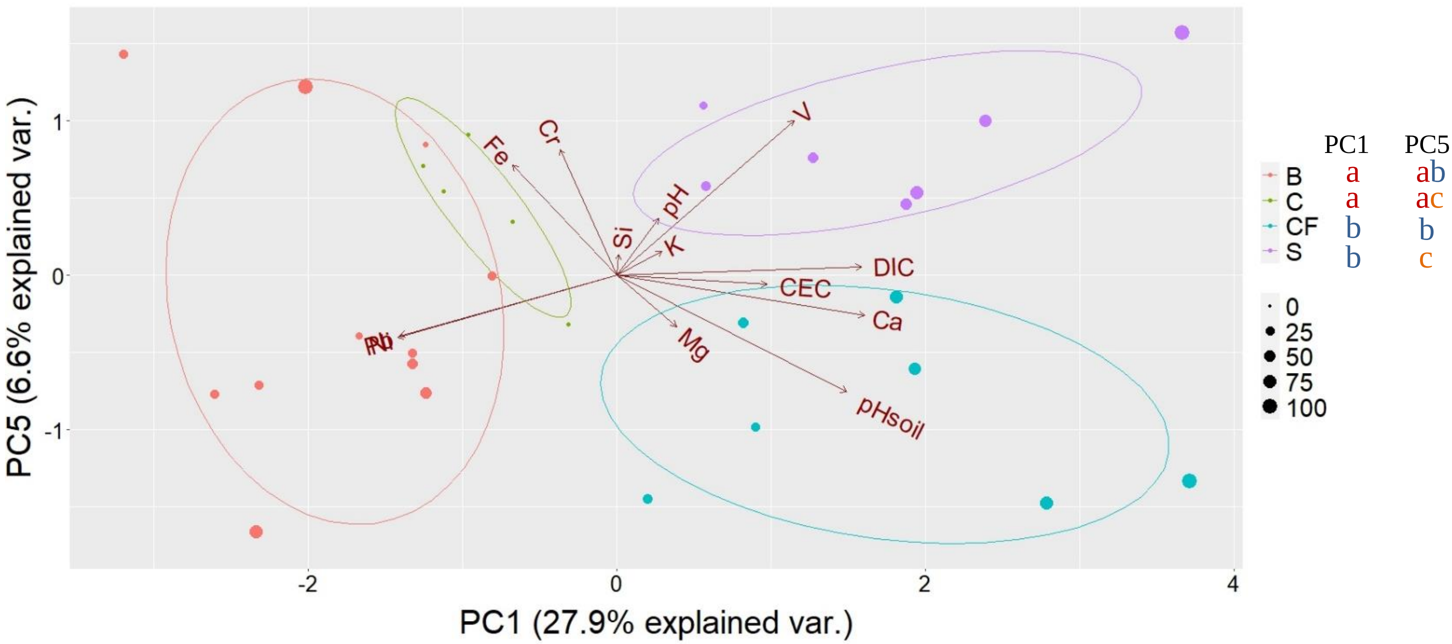

Figure 5: PC1 and PC5 of the principal component analysis with porewater nutrients (Ca, Fe, K, Mg, Si), toxic trace elements (Cr, Ni, Pb, V), porewater pH, soil pH, and soil CEC. Differences in PC1 and PC5 were found among silicate materials (B= Basalt, C= Control, CF= Concrete fines, S= Steel slag) by linear regression analysis with PC1 or PC5 as fixed variable and silicate treatment as covariable. Similar letters mean no statistically significant differences among the materials while different letters mean that PC1 or PC5 differed significantly among silicate materials, using a Tukey post-hoc test. P-and F-values are shown in Table S7.

The PCA-analysis showed a significant effect of silicate material on PC1 ($p<0.01$, $F=32.9$) and PC5 ($p<0.01$, $F=8.18$) (Fig. 5). PC1 is negatively correlated with porewater Pb and Ni concentrations, but positively with soil pH, CEC and DIC and porewater Ca and V concentrations. PC1 is significantly lower for basalt compared to concrete fines and steel slag (both $p<0.01$, Table S7). PC5 is negatively correlated with soil pH but positively with concentrations of Fe, Cr and V in the porewater. PC5 is significantly higher for steel slag compared to basalt ($p=0.03$) and concrete fines ($p<0.01$). While PC2 (positively correlated with Ca, Fe, Mg, Si, and K porewater concentrations, but negatively with soil CEC, porewater Cr and DIC) did not differ among the treatments, PC3 (negatively correlated with CEC, porewater Ni, Pb, and Mg) and PC4 (negatively correlated with porewater Cr and pH, and positively with porewater V concentrations) showed significant differences among treatments (Fig. 8, Table S7, Fig. S5). PC3 is significantly lower with basalt compared to the control, while PC4 is significantly higher with steel slag compared to concrete fines (Table S7, Fig. S5). The differences among concrete fines and steel slag were more prominent for PC5, which only explained 3.1% of the variance less than PC4 (Fig. 5, Fig. S5, TableS7).

3.2 Plant growth parameters

Although basalt application did not affect plant height and LAI, plant biomass increased with basalt application amount (Fig. 6, Fig. 7, Table S8). This increase was significant for the stem, tassel, total aboveground and root biomass, and borderline significant for the leaves (Fig. 7). Total aboveground biomass was significantly higher with basalt application compared to concrete fines and steel slag (Fig. 7, Table S9). Contrastingly, plant height increased over time with increasing concrete fines (almost statistically significant) and steel slag (statistically significant) application amount but LAI and stem, leaves, corn, and root biomass remained unaffected, and hence, total aboveground biomass did not change (Fig. 6, Fig. 7, Table S8). Nonetheless, tassel biomass increased significantly with both increasing application amounts of steel slag and concrete fines (Fig. 7).

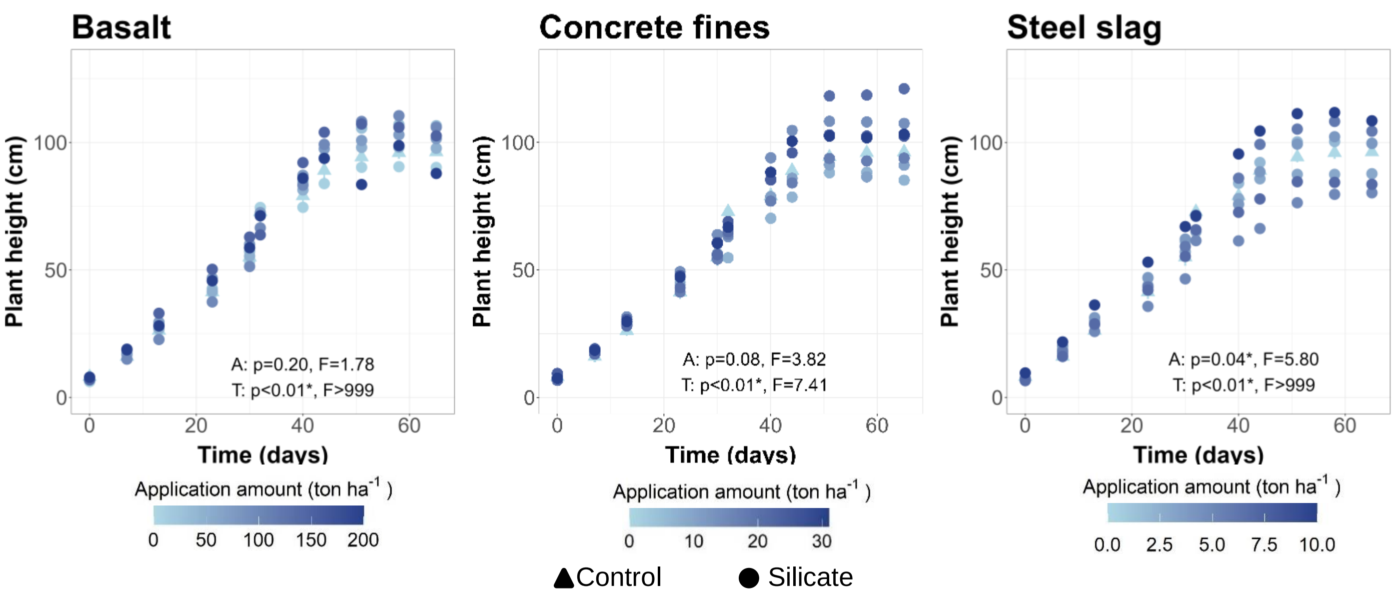

Figure 6: Plant growth during the experiment for basalt, concrete fines, and steel slag treatments. Control (0 ton ha $^{-1}$) and basalt treatment with an application rate of 50 ton ha^{-1} are averages of five replicates and are shown with standard error. The other treatments have one replicate. P-values and F-values are shown from a linear mixed model with plant height as the response variable and silicate application amount, time, and interaction as covariable. If the interaction was not statistically significant, this was deleted from the model and thus not shown here. Statistically significant relationships are indicated by an asterisk (*).

The aboveground/belowground ratio was unaffected by any treatments (Table S8). The model selected by the AIC method included K, Ca, Pb, and Cr concentrations in the soil porewater, and soil pH and CEC. Of these variables, total aboveground biomass was significantly positively correlated with soil porewater Ca ($p<0.01$, $F=3.47$) and Pb concentrations ($p<0.01$, $F=4.19$), and soil pH ($p=0.03$, $F=2.81$). The PCA analysis showed a significantly negative relationship between biomass and PC3, which is negatively correlated with CEC values and porewater Mg, Ni, and Pb concentrations (Fig. 8).

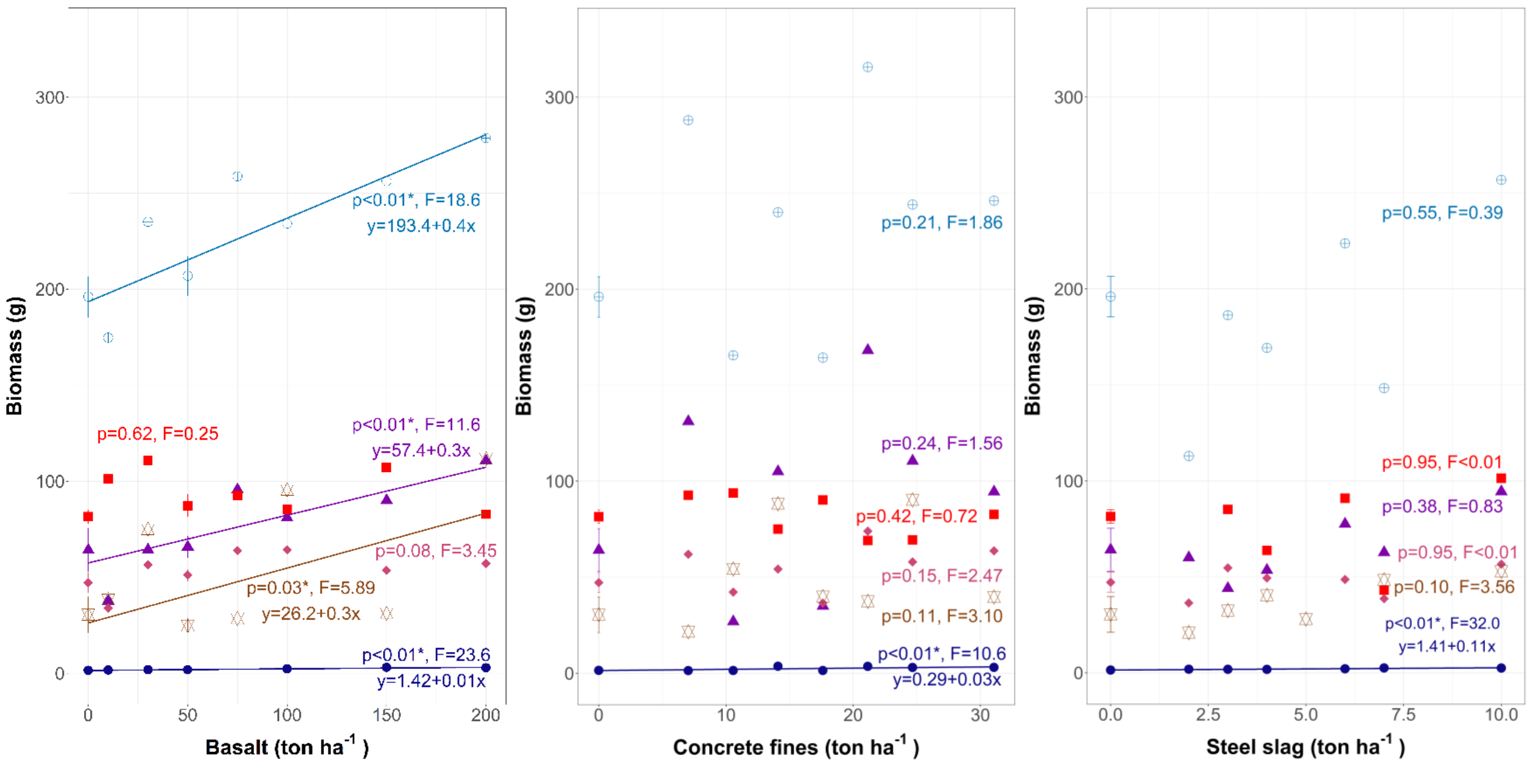

Figure 7: Biomass of the different plant parts (leaves, corn, tassel, stem) and total aboveground biomass of maize plants for basalt, concrete fines, and steel slag treatments. Control (0 ton ha $^{-1}$) and basalt treatment with an application rate of 50 ton ha^{-1} are averages of five replicates and are shown with standard error. The other treatments each have one replicate. P-and F-values are shown of a linear regression analysis with biomass as the response variable and concentration of the silicate material as covariable. Statistically significant regression is indicated by an asterisk (*), with equation and regression line.

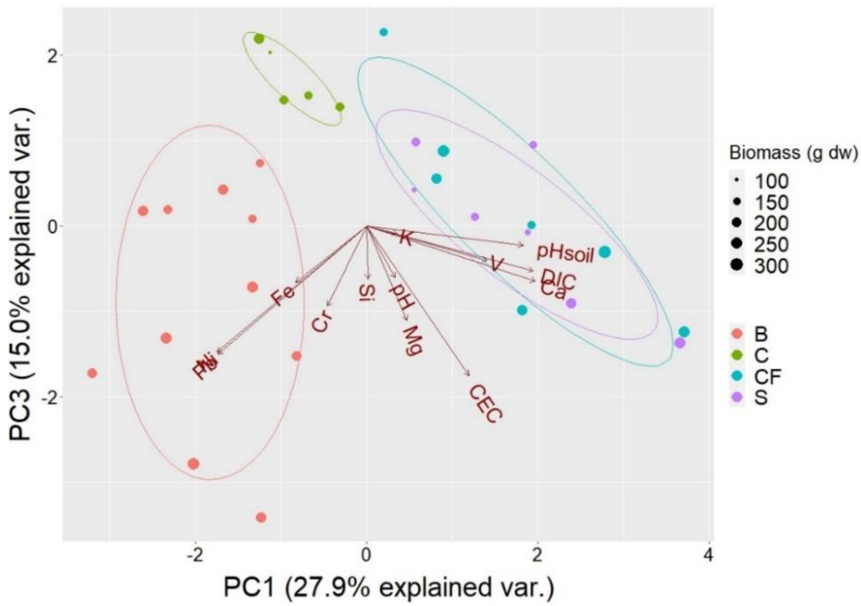

Figure 8: Scatter plot of PC1 and PC3 of the principal component analysis with porewater nutrients (Ca, Fe, K, Mg, Si), toxic trace elements(Cr, Ni, Pb, V), porewater pH, soil pH, and soil CEC. The sizes of the dots reflect the total aboveground biomass, which was significantly correlated with PC3. Different silicate treatments (B= Basalt, C= Control, CF= Concrete fines, S= Steel slag) are displayed in different colours.

3.3 Plant nutrients

Increased basalt application amount resulted in decreased Ca concentrations in the aboveground plant parts, but only significantly for the stem and the tassel. Root Ca concentrations, on the other hand, increased with increasing basalt application amount (Fig. 9), but these were generally lower with basalt than with concrete fines or steel slag application. Mg concentrations increased in the plant parts with increasing basalt application, albeit not statistically significant for the top leaf and the corn (Fig. 9). Root Mg concentrations were significantly higher with basalt compared to concrete fines and steel slags (Table S9). Basalt application did not significantly affect Fe and K concentration in any of the plant parts, and P concentration remained unaffected except for a significant increase in the tassel (Fig. 9). Basalt application had no significant impact on Si concentration in the top leaf, tassel, and roots. In stems, Si concentrations decreased with increasing application amount of basalt, while Si concentration increased in the corn (Fig. 9).

The C/N ratio of plant tissues was usually not affected by basalt application, although in the tassels, the C/N ratio decreased with increasing basalt application amount, while in the top leaf, the C/N ratio increased due to reduced N concentration (Fig. 10, Fig. S5). Total plant C stocks increased with increasing basalt application amount, while N stocks were not affected (Fig. S5). Furthermore, total plant Mg and K stocks increased with increasing basalt application amount, while Ca, P, and Si stocks remained unaffected (Fig. 11).

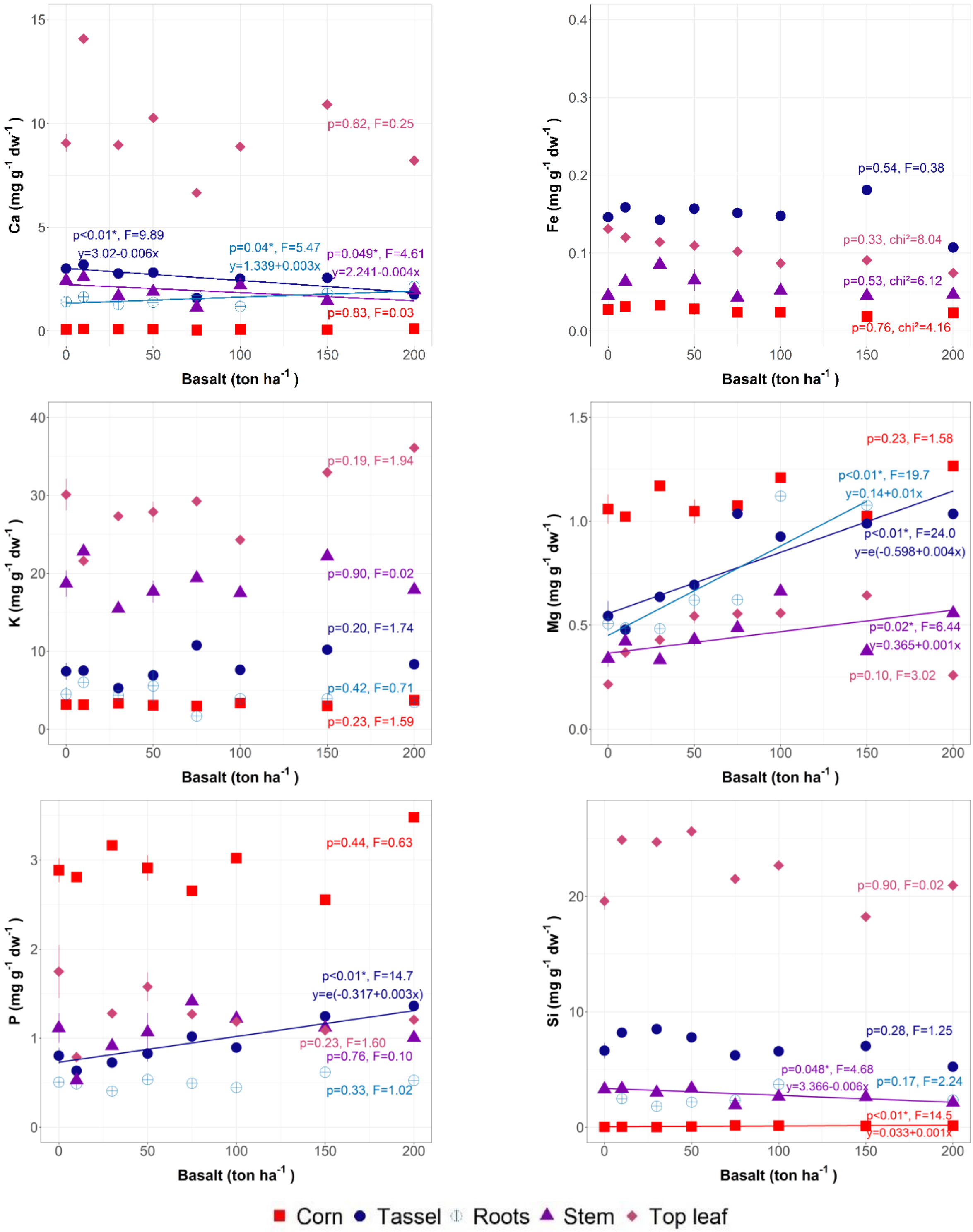

Figure 9: Concentrations of Ca, Fe, K, Mg, P, and Si in corn, tassel, roots, stem, and top leaf of the basalt treatment. Data of 0 and 50 ton ha^{-1} of basalt are averages of five replicates with standard error. Note that in some cases, the error bars are smaller than the symbol. The other application amounts each have one replicate. P-and F-values are shown of the linear model with elemental concentration as the response variable and silicate concentration as covariable. Statistically significant relationships are indicated with an asterisk (*), with equation and regression line.

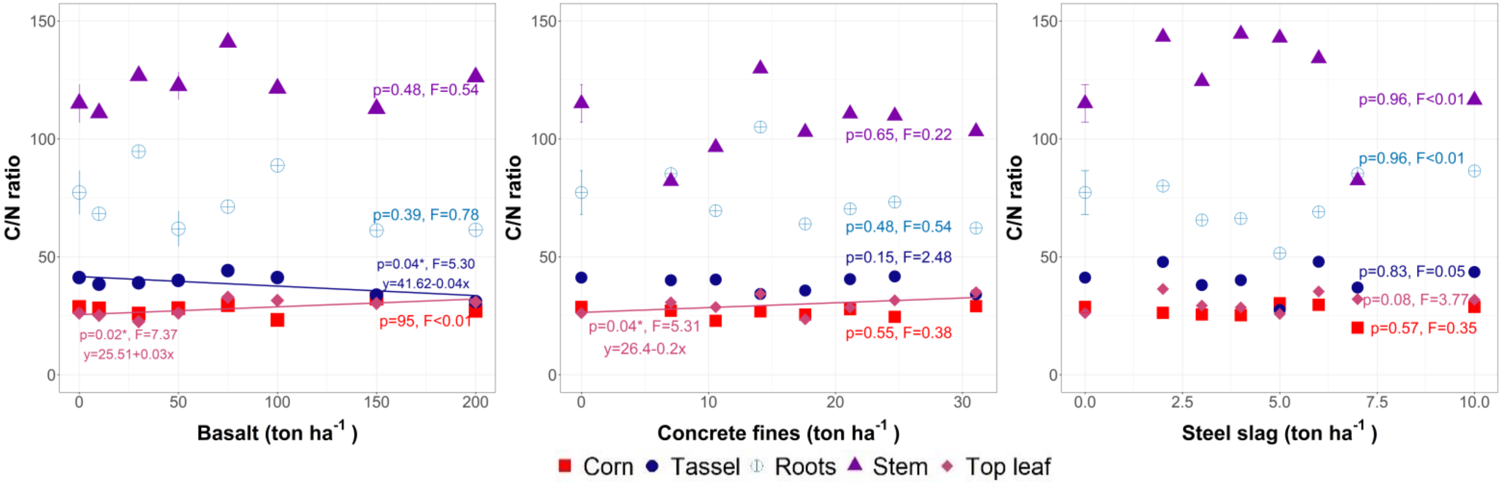

Figure 10: C/N ratio in corn, tassel, stem, top leaf, and roots of maize for the silicate treatments (basalt, concrete fines, steel slag). Data without silicates (0 ton ha^{-1}) and 50 ton ha^{-1} of basalt are an average of five replicates with standard error. Note that in some cases, the error bars are smaller than the symbol. The other treatments each have one replicate. P-and F-values are shown of the linear model with C/N ratio as the response variable and silicate concentration as covariable. Statistically significant relationships are indicated with an asterisk (*), with equation and regression line.

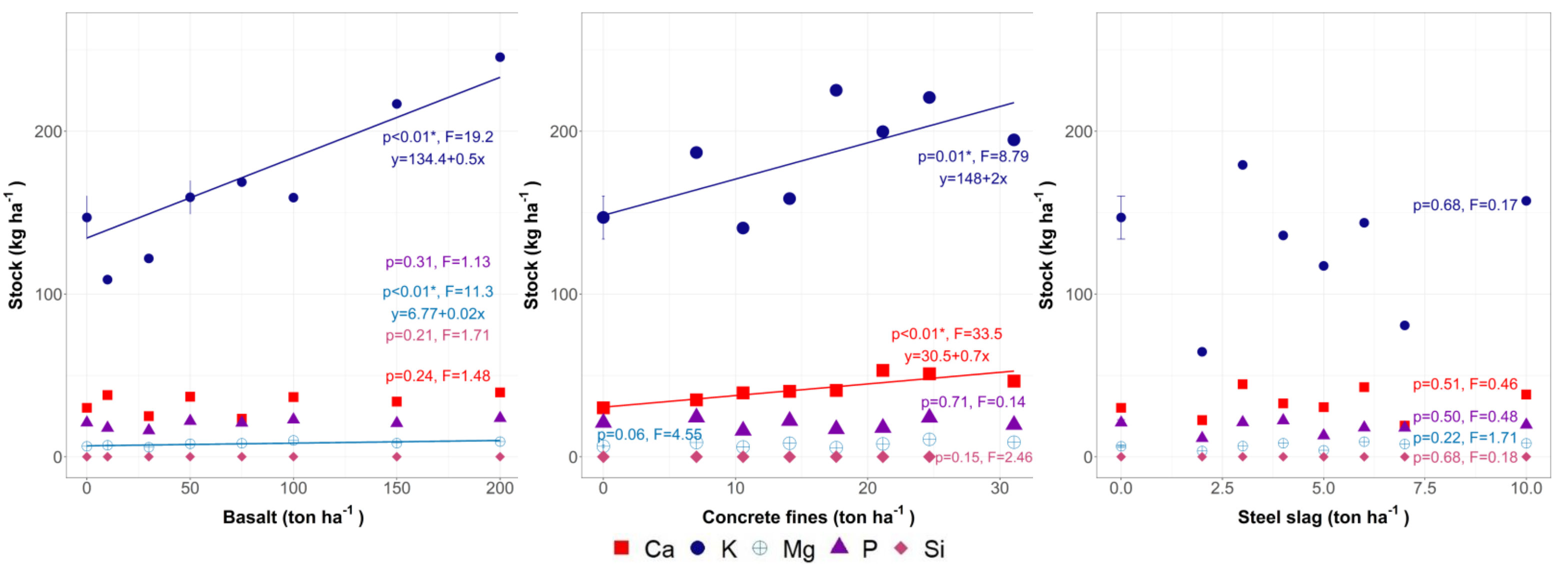

Figure 11: Stocks of Ca, K, Mg, P, and Si in the crops for the silicate treatments (basalt, concrete fines, steel slag). Data without silicates (0 ton ha^{-1}) and 50 ton ha^{-1} of basalt are an average of five replicates with standard error. Note that in some cases, the error bars are smaller than the symbol. The other treatments each have one replicate. P and F-values are shown of the linear model with stocks as the response variable and silicate concentration as covariable. Statistically significant relationships are indicated with an asterisk (*), with equation and regression line.

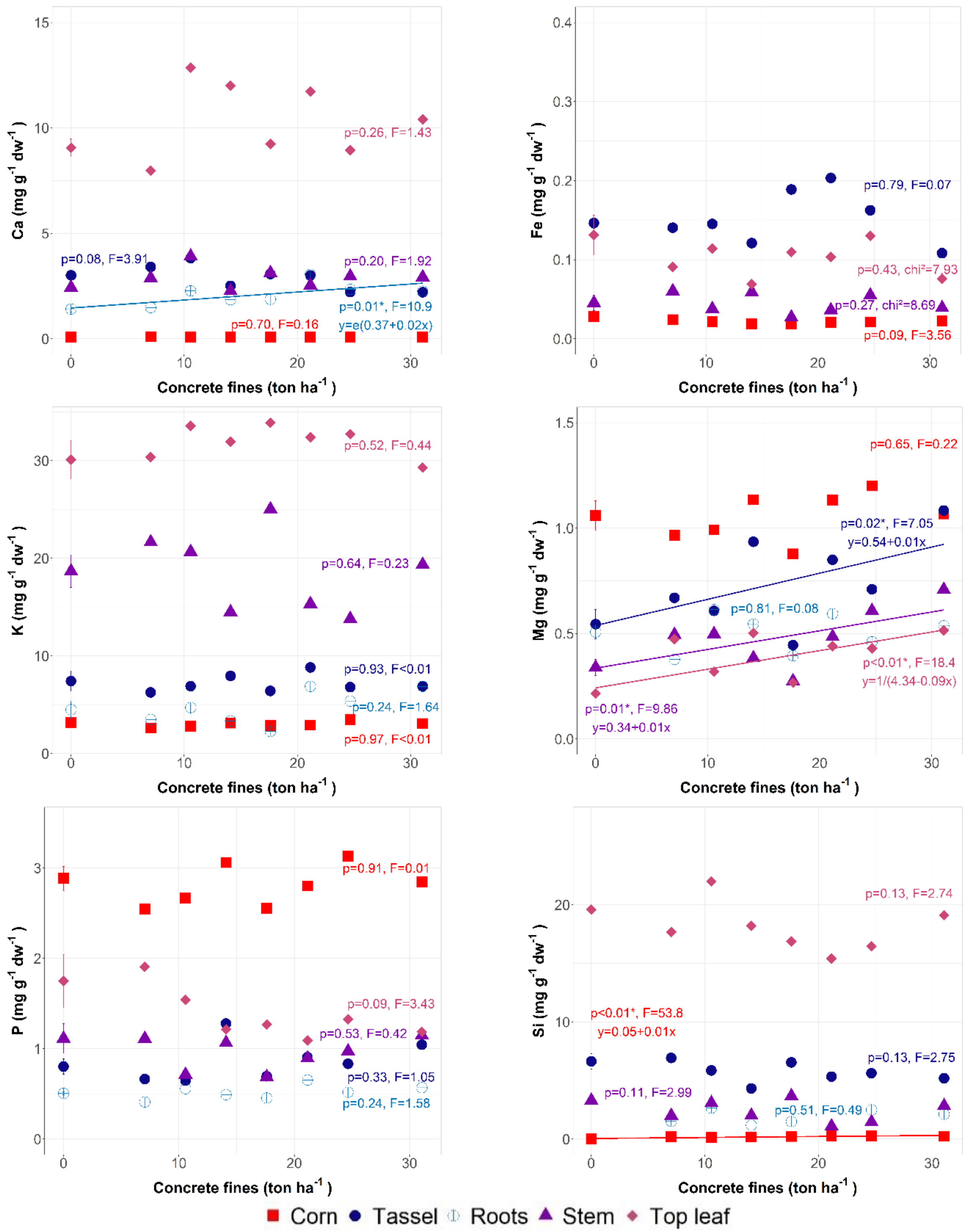

Figure 12: Concentrations of Ca, Fe, K, Mg, P, and Si in corn, tassel, roots, stem, and top leaf of the concrete fines treatment. Data of the control treatment (0 ton ha^{-1}) is an average of five replicates with standard error. Note that in some cases, the error bars are smaller than the symbol. The other application amounts each have one replicate. P-and F-values are shown of the linear model with elemental concentration as the response variable and silicate concentration as covariable. Statistically significant relationships are indicated with an asterisk (*), with equation and regression line.

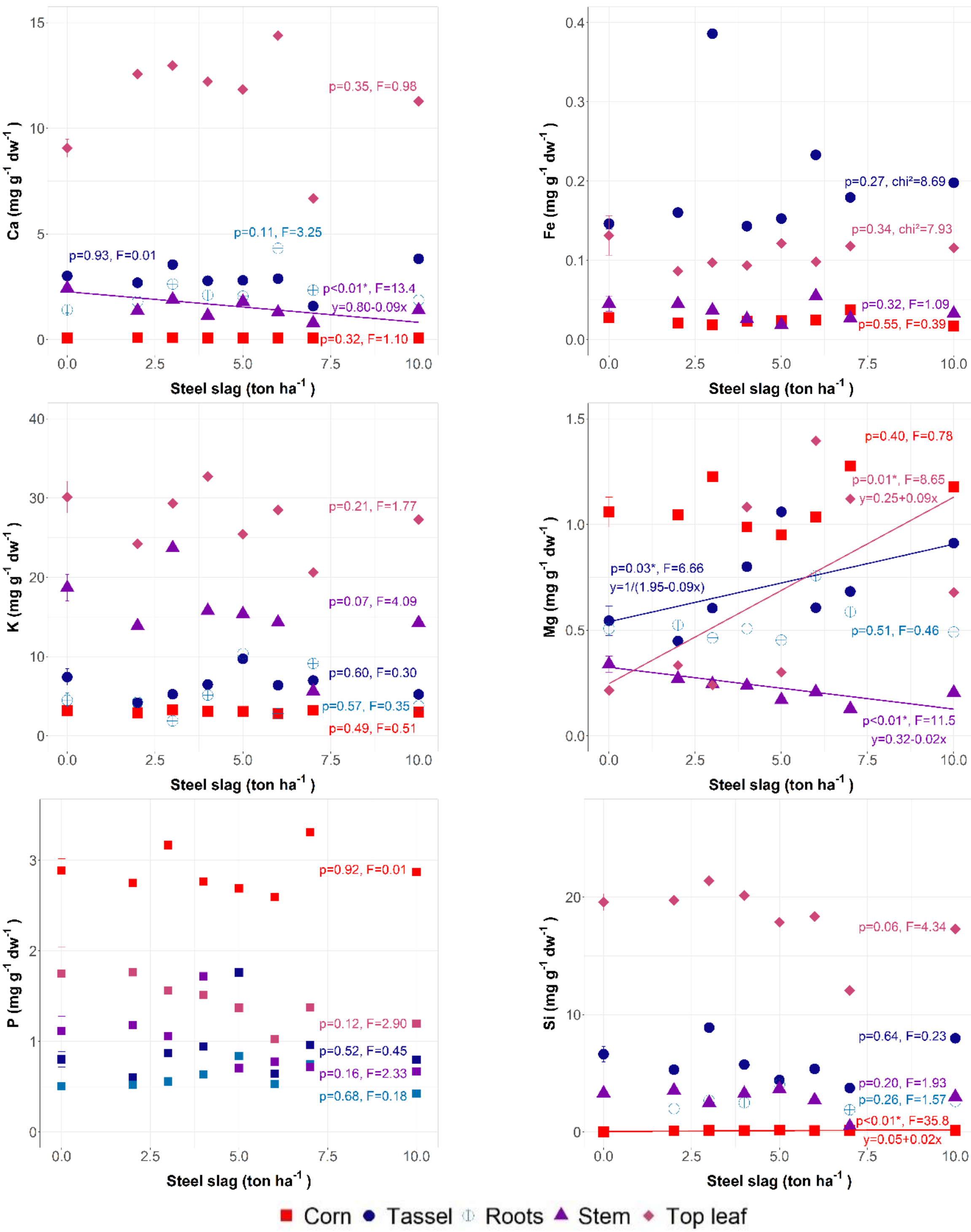

Figure 13: Concentrations of Ca, Fe, K, Mg, P, and Si in corn, tassel, roots, stem, and top leaf of the steel slag treatment. Data of the control treatment (0 ton ha^{-1}) is an average of five replicates with standard error. Note that in some cases, the error bars are smaller than the symbol. The other application amounts each have one replicate. P-and F-values are shown of the linear model with elemental concentration as the response variable and silicate concentration as covariable. Statistically significant relationships are indicated with an asterisk (*), with equation and regression line.

Concrete fines application did not affect plant Ca concentrations, except for significantly increased root Ca concentration and a tendency of decreased tassel Ca concentrations ($p=0.08$) (Fig. 12). Stem Ca concentrations were higher with concrete fines compared to basalt and steel slag (Table S10). Mg concentrations increased with increasing concrete fine application amount, albeit not statistically significantly in the corn and roots (Fig. 12). Corn Si concentrations increased as well with concrete fines, and were higher than with basalt and steel slag (Fig. 12, Table S10). Concrete fine application did not affect plant Fe, K, and P concentrations. The C/N ratio significantly increased in the top leaf, even though C and N concentrations were not significantly affected by concrete fines (Fig. 12, Fig. S4). In the other plant parts, the C/N ratio remained unaffected (Fig. 12). Total plant C stocks increased significantly with increasing application amount of concrete fines, whereas total plant N stocks were not affected (Fig. S6). Plant P and Si stocks were not influenced by concrete fines application amounts, while Ca, K, and Mg stocks increased with concrete fines, albeit only statistically significantly for Ca and K (Fig. 11).

Steel slag application did not affect plant Ca concentrations, except for decreased stem Ca concentrations (Fig. 13). In leaves and tassels, Mg concentrations significantly increased with steel slag application amount, while it decreased in the stems (Fig. 13). Stem Mg concentrations were also lower with steel slag application than with basalt or concrete fines (Table S10). Corn and root Mg concentrations were not affected (Fig. 13). Steel slag application did not influence Fe, K, P, or Si concentrations in the plants except for increased corn Si concentrations with increasing steel slag application amount (Fig. 13). Leaves Si concentrations were higher with steel slag compared to basalt and concrete fines (Table S10). The C/N ratios in the plant parts remained unaffected by steel slag application (Fig. 10), even though stem N and top leaf C concentrations decreased (Fig. S5). Total plant C and N stocks (Fig. S6) and Ca, Mg, P, K, and Si stocks (Fig. 11) remained unaffected by steel slag application.

3.4 Toxic trace elements

In all corn samples and in over 85% of the stem samples, Pb was below the LOQ (0.1 mg kg^{-1} dw) and thus could not be statistically analysed. Pb was only detected in one control treatment and three basalt treatments (Table S6). Corn Cd concentrations were below LOQ (0.015 mg kg^{-1} dw) in all samples of the steel slag treatment and was only detected once with concrete fines and once with basalt application (Table S6). Basalt application did not significantly affect toxic trace element concentration in the plant parts, except for decreasing Cd (statistically significant), with the largest decrease of 54% when 75 ton basalt ha^{-1} was applied, and V (borderline significant) concentrations in the top leaf (Fig. 14).

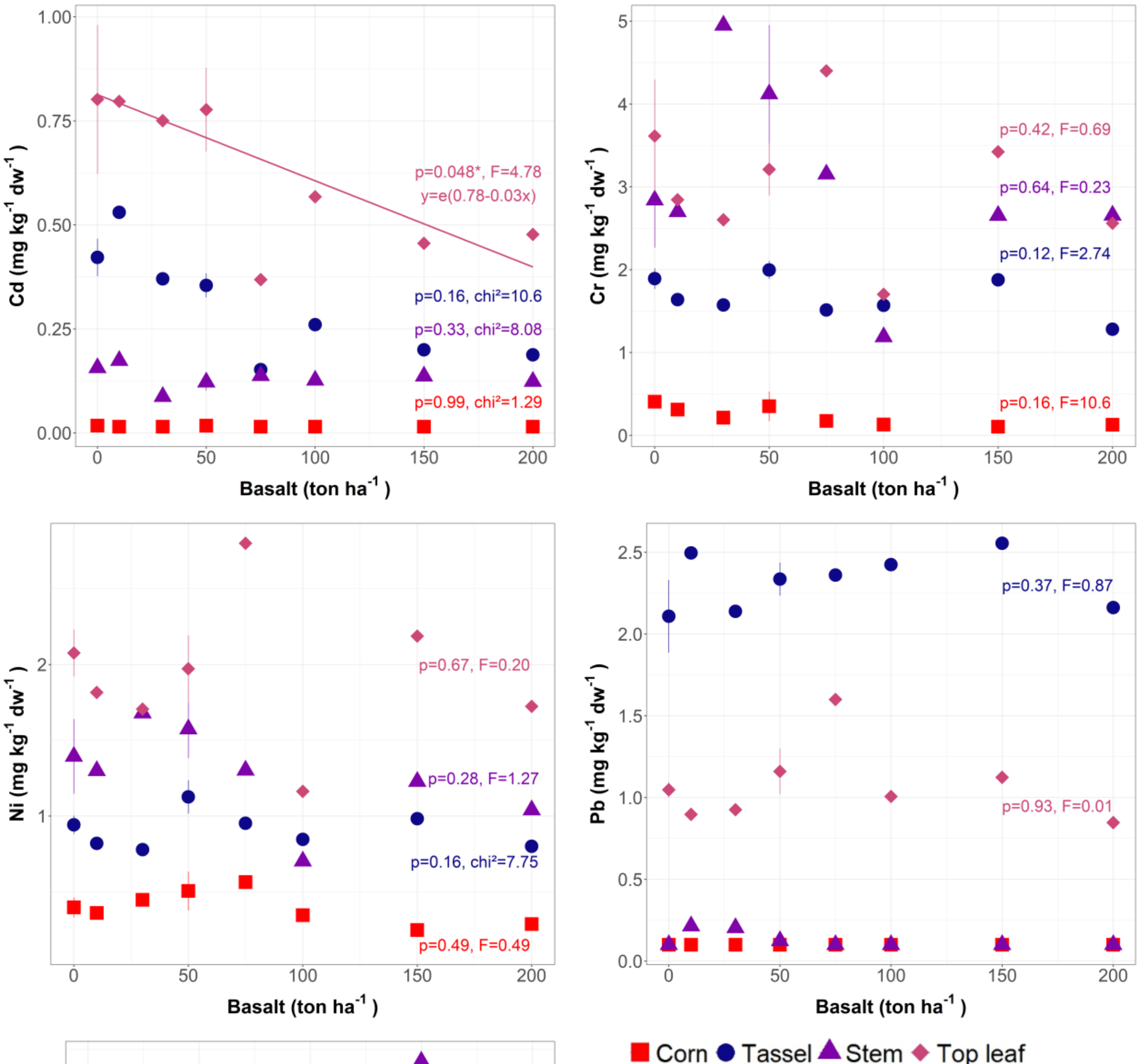

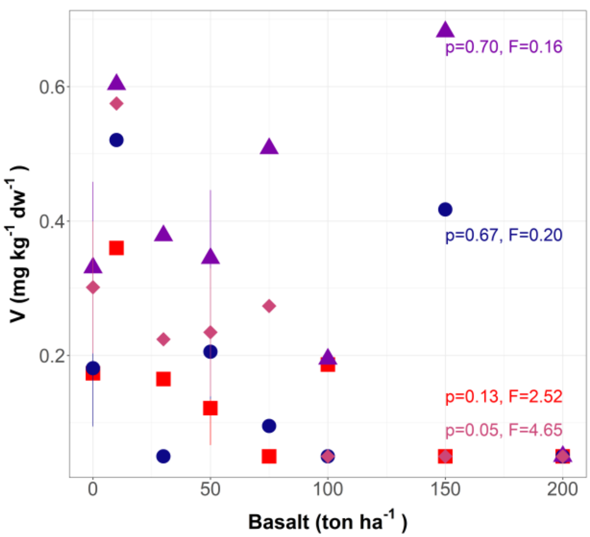

Figure 14: Concentrations of Cd, Cr, Ni, Pb and V in corn, tassel, stem and top leaf of the basalt treatments. Data of 0 and 50 ton ha^{-1} of basalt are an average of five replicates with standard error. Note that in some cases, the error bars are smaller than the symbol. For 10, 25, 75, 100, 150, and 200 ton ha^{-1} of basalt, there is one measurement each. P-and F-values are shown of the linear model with toxic trace element concentration as the response variable and silicate concentration as covariable. Statistically significant relationships are indicated with an asterisk (*), with equation and regression line.

Concrete fine application generally decreased plant Cr concentrations, albeit only significantly in corn and tassel (Fig. 15), with a maximum decrease of 81% with the highest application amount, and 46% for 10.57 ton ha^{-1} of concrete fines, respectively. Additionally, tassel Cd concentrations decreased with increasing concrete fines application amount, while Cd concentrations in the other plant parts remained unaffected. Corn Ni concentrations decreased significantly with a maximum decrease of 60.8% when 21.15 ton ha^{-1} of concrete fines was applied, and a non-significant trend of decreased stem Ni concentrations was observed with increasing concrete fine application amount, while Ni concentration was unaffected in the other plant parts (Fig. 15). Plant Pb concentrations were not affected by concrete fines application, and neither were plant V concentrations, except for a decrease observed in the top leaf (Fig. 15).

Apart from decreased Cd concentrations in the stem (statistically significant) and in tassels (borderline significant), Cd levels were not affected by steel slag application (Fig. 16). Stem Cd concentrations were lower with steel slag compared to basalt and concrete fines (Table S11). Furthermore, steel slag application decreased corn Cr concentrations, up to 83% with an application amount of 3 ton ha^{-1} of steel slag. No influence was observed in the other plant parts. V and Pb concentrations were not affected by steel slag application, except for an increase observed in the top leaf (Fig. 16). With the highest application amount of steel slag, Pb concentrations increased by 47% compared to the control treatment.

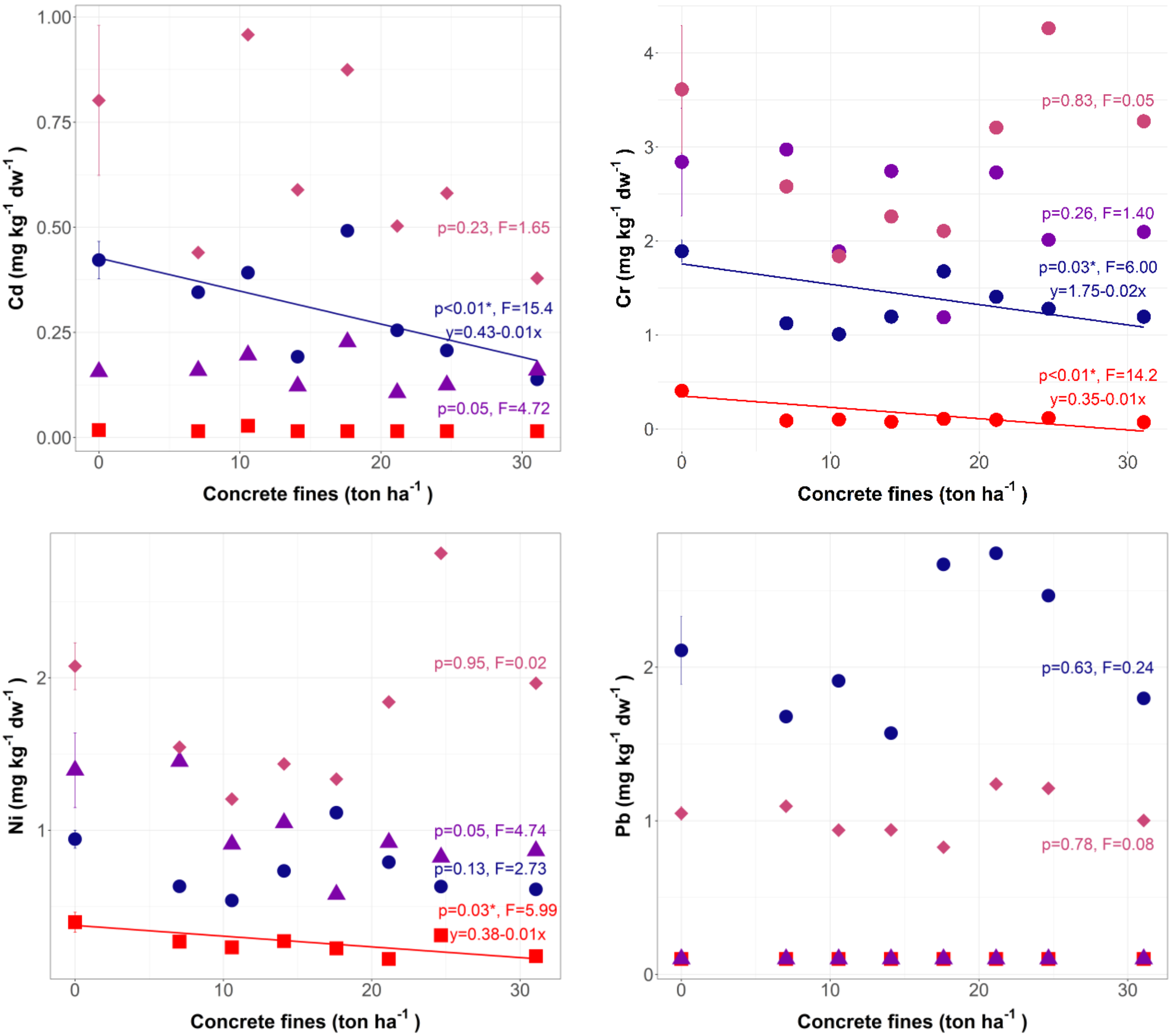

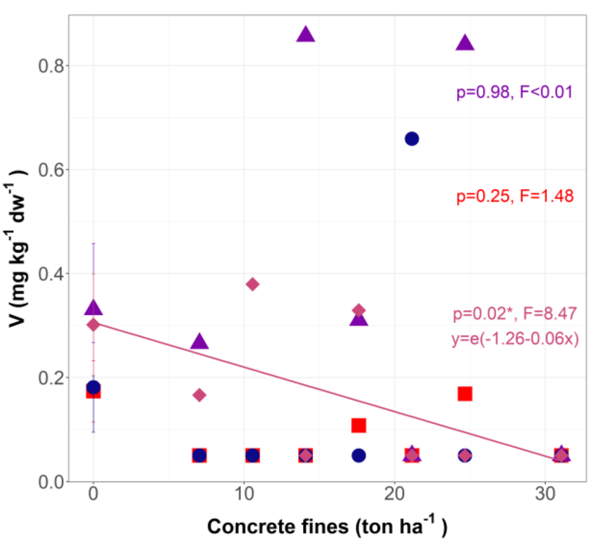

Figure 15: Concentrations of Cd, Cr, Ni, Pb, and V in corn, tassel, stem, and top leaf for the concrete fines treatments. Data of 0 ton ha^{-1} of concrete fines is an average of five replicates with standard error. Note that in some cases, the error bars are smaller than the symbol. For 7.04, 10.57, 14.09, 17.62, 21.15, 24.67 and 31.07 ton ha^{-1} of concrete fines, there is one measurement each. P-and F-values are shown of the linear model with toxic trace element concentration as response variable and silicate concentration as covariable. Statistically significant relationships are indicated with an asterisk (*), with equation and regression line.

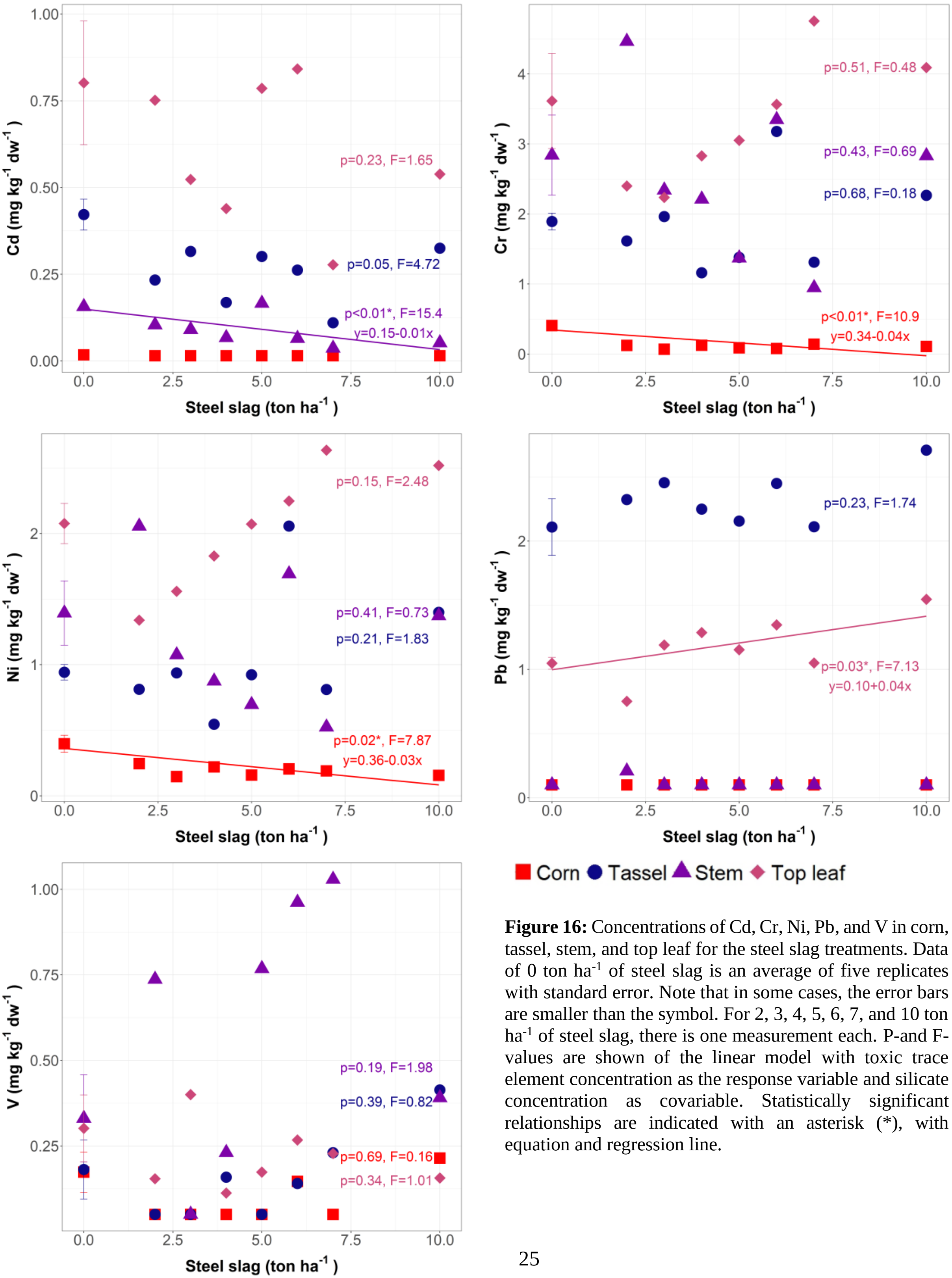

Figure 16: Concentrations of Cd, Cr, Ni, Pb, and V in corn, tassel, stem, and top leaf for the steel slag treatments. Data of 0 ton ha^{-1} of steel slag is an average of five replicates with standard error. Note that in some cases, the error bars are smaller than the symbol. For 2, 3, 4, 5, 6, 7, and 10 ton ha^{-1} of steel slag, there is one measurement each. P-and F-values are shown of the linear model with toxic trace element concentration as the response variable and silicate concentration as covariable. Statistically significant relationships are indicated with an asterisk (*), with equation and regression line.

4. Discussion

4.1 Silicate weathering and soil properties

The DIC and base cations such as Ca^{2+} and Mg^{2+} in the porewater provide an indication of the weathering rate of the added silicate minerals (Haque et al., 2019; Kelland et al., 2020). As expected, increases in DIC were lowest for basalt compared to concrete fines and steel slag, indicating a higher weathering rate for the latter two silicates. This was accompanied by a higher initial increase of soil and porewater pH for steel slag and concrete fines. Concrete fines used in this study contained about 18% calcite, and steel slag about 9%. Calcite weathers faster than silicate minerals (Berner et al., 1983; Lehmann et al., 2023), potentially explaining the higher increase in DIC with concrete fines and steel slag compared to basalt, as basalt does not contain calcite. Even though the CO_2 removal of these silicates is not part of the current study, we want to emphasize that calcite weathering does not contribute to long-term carbon capture, and has a risk of reversal if carbonates reprecipitate downstream after leaching (Berner et al., 1983; Lehmann et al., 2023). In other words, the higher increase in weathering products with concrete fines and steel slag in our experiment does not imply a proportionate increase in CO_2 removal. EW studies have consistently shown increases in DIC and pH as well following silicate application, whether using a mixture of rock types (Guo et al., 2023), basalt (Buckingham & Henderson, 2024; Conceição et al., 2022), or steel slag (Buckingham & Henderson, 2024).

Moreover, the release of Mg and Ca increased with application amounts of the silicates, as evidenced by soil porewater, PRS probes, and plant measurements, and this is in line with other experiments (Amann et al., 2020; Buckingham & Henderson, 2024; Guo et al., 2023; Vienne et al., 2022; Yan et al., 2023). Soil porewater Si concentrations increased as well in our study (Fig. 3), similar to previous studies (e.g. Buckingham & Henderson (2024); Guo et al. (2023); Vienne et al. (2022)). The observed variability in nutrient concentrations, especially Si, for the control treatment and the 50 ton ha^{-1} of basalt is likely due to local differences in soil conditions and fluctuations in porewater chemistry. Despite this variability, significant differences among treatments were identified. However, because this study did not include replicates for the other application amounts, the extent of variability could not be confirmed.

In contrast, Fe was unaffected and even decreased with application of concrete fines. The latter may be attributed to the increased pH, which can stimulate the formation of insoluble Fe compounds, reducing Fe availability (e.g. Lindsay et al. (2008); Shenker & Chen (2005)). Basalt and steel slag contain more Fe compared to concrete fines (see Table 2) and may have supplied sufficient Fe to counterbalance decreases in Fe as a result of increased pH.

The silicate materials in our study contained toxic trace elements which can also be released. Given their known toxicity for plants (Nagajyoti et al., 2010), it is imperative to assess the associated risks of toxic trace element pollution when considering EW in agriculture. Indeed, porewater concentrations of Cr, Ni, Pb and V increased in some of our treatments.

Increased porewater Ni concentrations with basalt and higher porewater Cr concentrations with steel slag can be explained by the material composition (Table 2). On the other hand, porewater V concentrations also increased with increasing amount of concrete fines, which did not contain V. Porewater V concentrations were thus not only influenced by the release of V from the silicates (as they also increased with steel slag, that do contain V), but also by changes in soil properties. As V is more mobile with increasing pH (Chen et al., 2021), we presume that the increased pH (Fig. 2) increased porewater V concentrations. Availability of Pb is generally also controlled by soil pH. At higher pH, Pb is less available for plants (Kushwaha et al., 2018). Despite basalt lacking Pb, and the rise in soil pH, porewater Pb concentrations increased with increasing basalt application. This unexpected increase may be related to competition for soil binding sites, with the released Ca increasingly out-competing Pb due to their similar size and reactivity (Klitzke & Lang, 2009; L. Li et al., 2014).

4.2 Plant growth

Plants can benefit from EW because it can create a more favourable environment (Calabrese et al., 2022; Kelland et al., 2020). Indeed, basalt application increased aboveground and belowground biomass. These findings are consistent with observations of tropical systems (Swoboda et al., 2022). Also in temperate climates, basalt has been reported to increase agricultural yield (Kelland et al., 2020; Skov et al., 2024), but other studies found no significant effect (Vienne et al., 2022). Furthermore, increased root biomass with basalt application may indicate higher belowground C inputs by plants, but can also increase microbial activity leading to accelerated soil organic matter decomposition, which can impact soil organic C stocks (Fu & Cheng, 2002; Kögel-Knabner et al., 2022; Kuzyakov, 2002).

In contrast to basalt, concrete fines, and steel slag application did not affect plant biomass, except for increased tassel biomass. Previously, the application of steel slag has been shown to have varying effects on crop growth. In a tropical climate, soybean yield increased with steel slag application in two consecutive crop cycles (Deus et al., 2020). Similarly, Wang et al. (2015) reported an initial increase in rice yield upon steel slag application on a paddy field, but this effect diminished after two growing seasons. Pistocchi et al. (2017), on the other hand, reported a decrease in wheat yield, while tomato yield increased over three growing seasons upon steel slag application in slightly alkaline loamy sand soils.

In our study, differences in plant biomass were significantly correlated to differences in soil pH, and pH may thus (partly) explain the biomass response. The optimal pH for maize growth is between 5.5 and 7.5 (Lizárraga-paulín et al., 2011), a threshold that was surpassed early in the growing season for the highest application amounts of concrete fines and steel slag, but not for basalt (Fig. 2). We therefore presume that the pH was more conducive across the spectrum of basalt application amounts, thereby increasing the plant biomass. This postulation is supported by the PCA analysis, as soil pH was one of the major variables affecting both PC1, which separated the control and basalt treatment from the concrete fines and steel slag, and PC5, which separated the concrete fines and the steel slag treatments. However, plant biomass only differed significantly between basalt and steel slag application, and not compared to concrete fines. The high variation in biomass with concrete fines application precludes drawing firm conclusions. Even though the substantial pH increase may have limited the positive plant growth response with steel slag application, no adverse effects were detected.

4.3 Nutrient status of the plants

Nutrient release from silicate weathering is expected to stimulate plant growth and biomass, with nutrient release varying based on material composition. We expected the same differences in plant stoichiometry, and indeed, plant nutrient concentrations aligned with the soil Si and Mg measurements; corn Si and plant Mg concentrations increased with silicate application. However, with basalt application, plant Ca concentrations even decreased in some plant parts and are thus not in line with plant availability of Ca, presumably because of competition between Mg and Ca. The Ca/Mg ratio in soil porewater decreased with basalt (Fig. S7). This has previously been related to reduced plant Ca concentration (Kopsell et al., 2013; Osemwota, 2007). A similar trend of increasing Mg and decreasing Ca concentrations was found with dunite application in wheat and barley (Rijnders et al., 2023) and ryegrass (Ten Berge et al., 2012).

The three silicate materials contained Mg, resulting in higher porewater Mg and plant Mg concentrations. Mg is an essential plant nutrient that is crucial for various physiological functions, including protein and chlorophyll synthesis, enzyme activation and ATP synthesis, and regulatory processes of photosynthesis (Hawkesford et al., 2012). Mg deficiency often arises in agricultural systems with imbalanced crop fertilization with N, P, and K, primarily due to competition between Mg and other ions, particularly K and Ca (Guo et al., 2016). The increased Mg availability and plant concentrations indicate that fertilization with silicate minerals can aid in restoring Mg availability in agricultural soils. Our results correspond to previous experiments employing basalt rocks. Boniao et al. (2002), for example, showed that corn height and biomass increased after basalt amendment and this was correlated with Mg concentration in soil porewater. Similarly, in Cameroon, maize cultivation utilizing three local basalts revealed the largest yield benefit for the basalt with the highest Mg and Ca content, despite its lower K and P content (Tchouankoue, 2014). Additionally, other minerals, like the Mg-silicate dunite, also increased Mg concentrations in wheat and barley (Rijnders et al., 2023).

Even though not considered an essential plant nutrient, Si can protect the plant from (a)biotic stresses by making the plant structure more rigid and stronger (Bhatt & Sharma, 2018). Additionally, Si interacts with several key components of stress signalling pathways of plants (Majeed et al., 2019), which can stimulate crop growth especially when plants are experiencing stress. Indeed, studies where steel slag increased rice (Ning et al., 2014) and soybean (Deus et al., 2020) yields also reported increased plant Si concentrations. In our study, the plants did not experience any noticeable stress, which may explain why Si concentrations were not related to increased plant biomass.

Unlike Ca, Mg, and Si, plant concentrations of P, K, and Fe were not much affected by silicate application. Despite decreased K availability with concrete fines and steel slag, plant K concentrations remained unaffected. The simultaneous increase in K stocks following the application of basalt and concrete fines suggests that K was sufficiently available across all treatments. While this contrasts with a few earlier studies that did report increased plant K concentration upon silicate addition (Skov et al., 2024; Ten Berge et al., 2012), our result is in line with the study of (Rijnders et al., 2023), where the application of 220 ton ha^{-1} of dunite did not affect P and K concentrations in wheat and barley. Plant Fe concentrations also remained unaffected by silicate application, despite a decrease in Fe in soil porewater with concrete fines. Fe is relatively immobile, and symptoms of Fe deficiency typically appear on the new leaves. However, the lowest leaf Fe concentration measured in our study was 0.07 mg g^{-1} dw (=70 ppm), which falls perfectly above the minimum threshold of Fe concentrations in young leaves (i.e., 30 ppm Fe on a dry-weight basis; (Hochmuth et al., 2012)). Therefore, we can assume that sufficient Fe was available, even though plant available Fe decreased with concrete fines. In an experiment of Wang & Qing-sheng (2006), Fe did not increase as well with their lowest steel slag application amount (44 ton ha^{-1}), using sandy loam soil.

Furthermore, plant available N did not change with silicate application. While plant N concentration slightly changed with basalt and steel slag application (Table S3), plant N stocks remained unaffected. This was expected since the silicates lack N and every treatment received the same input of N fertilizer. However, the C/N ratio within leaf tissues increased with basalt and concrete fines application, suggesting higher C assimilation rate per unit of N, indicating improved N use efficiency or N limitation (Schlüter et al., 2012). Given the biomass increase with basalt and no decrease with concrete fines, the elevated C/N ratio does not indicate N limitation, particularly given that the mesocosms received the same amount of N fertilization.

4.4 Plant toxic trace elements

In addition to nutrients, silicate weathering can be accompanied by toxic trace element release, raising concerns about toxic trace element contamination. The primary risks associated with basalt are Al, Cr and Ni, while concrete fines contain only Al in a substantial amount, and steel slag contain various toxic trace elements, with notable risks linked to Al and Cr. Despite the release of toxic trace elements from silicate weathering, concentrations of these elements in plant tissues were not affected or even decreased with increasing silicate application amount. This is similar to a previous study where dunite application did not affect most toxic trace elements and even decreased Ba and Sr concentrations in wheat and barley (Rijnders et al., 2023). Deus et al. (2020) also found that steel slag application did not affect toxic trace element concentrations in soybean, probably related to the increase in soil pH. Furthermore, basalt application did also not increase concentrations of Cd, Cr, Ni, and Pb in spring oats (Skov et al., 2024).

In this study, Cd, Cr, and V decreased in the plant parts with increasing silicate application. Decreases in Cd concentration were presumably a consequence of reduced Cd solubility following the pH increase with silicate application. Similar to our results, He et al. (2020) reported a decrease in Cd solubility and subsequent reduction in Cd concentrations in rice following steel slag amendment. In contradiction to our hypothesis, plant V concentrations did not increase in our experiment (and even decreased with concrete fines), despite elevated V concentrations in the soil porewater. Although V availability increases with pH, its uptake by roots decreases as the soil pH increases (Roychoudhury, 2020). Moreover, V that is taken up by plant roots will be predominantly retained in root tissue, particularly in cell walls where multiple proteins and polysaccharides form chelates with heavy metal ions (Aihemaiti et al., 2020; Roychoudhury, 2020), hence reducing its accumulation in aerial plant parts (Aihemaiti et al., 2020). This is similar for Cr, which may explain the decreased Cr concentrations in the above-ground plant parts (Ertani et al., 2017). Pistocchi et al. (2017) demonstrated that V and Cr indeed accumulated in the roots of tomato plants without translocation to the aerial plant parts after application of steel slag.

Furthermore, increased porewater Ni concentrations upon basalt application did not translate into increased Ni concentrations in the plant, presumably due to its uptake competition with other essential ions by plant roots (Sreekanth et al., 2013; Yusuf et al., 2011). This is similar to what was found by Vienne et al. (2022), where basalt application did not increase Ni concentrations in potatoes. Ni is a crucial component of many enzymes, and its deficiency can reduce plant growth but can be toxic for plants at elevated concentrations (Yusuf et al., 2011). Nevertheless, the toxicity level for sensitive species (10 mg kg^{-1} dw) was not exceeded in our study (Yusuf et al., 2011). In contrast, top leaf Pb concentrations increased with steel slag application, but these remained below the maximum allowable level of 0.05 mg kg^{-1} ww that has been set for corn (WHO & FAO, 2022), ranging from $0.58*10^{-6}$ to 0.03 mg kg^{-1} ww for all of the plant parts, and for the corn grains from $0.64*10^{-4}$ to $0.6*10^{-3}$ mg kg^{-1} ww. The one-time steel slag application up to 10 t ha^{-1} in our experiment did thus not pose a problem of toxic trace element contamination.

While at first sight reduced toxic trace elements in the plant may be beneficial for crop production, increased porewater concentrations, potential accumulation in the plant roots, and the immobilization of these elements in the soil may pose an environmental risk in the longer term. Our short-term experiment did not allow for complete weathering of the silicate materials, and increased release of toxic trace elements may thus occur still over longer time (Dupla et al., 2023). Furthermore, future decreases in soil pH may re-release these elements into the environment (Kicińska et al., 2022). This way, the toxic trace elements could gradually leach through the soil into the ground water, potentially posing a risk to water quality and human health (P. Li et al., 2021; Sbai et al., 2024).

5. Conclusion

In our mesocosm experiment, we investigated the influence of a range of application amounts of basalt, concrete fines, and steel slag on the growth, nutrient status, and toxic trace elements in *Zea Mays*. Basalt application increased plant biomass, while plant biomass was not affected by concrete fines and steel slag. Differences in plant biomass are presumably due to exceedance of the optimal soil pH early in the growing season for the highest application amounts of concrete fines and steel slag, but not with basalt. However, despite the limited effect on crop growth, plants were not negatively affected by silicate application.

Silicate application increased soil pH, and porewater Ca, Mg, and Si availability which translated into increased plant Mg and Si concentrations. Plant Ca concentrations also increased with concrete fines and steel slag application, while a decrease in stem Ca was observed for basalt. This difference was probably related to the Ca/Mg ratio of the rock. Consistent with previous studies, toxic trace element concentrations did not increase or even decreased in the aboveground plant parts with silicate application, even though the silicate materials contained and released these elements. Only leaf Pb increased with steel slag application and reached a concentration of up to 0.03 mg Pb kg^{-1} ww, which is still below the maximum level of 0.05 mg kg^{-1} ww of corn, set by the WHO. Moreover, Pb concentration in the corn grains was always below the LOQ. We therefore conclude that, in our experiment, crops mostly benefited from silicate application, with the largest benefits observed for basalt application. We did not find concerning toxic trace element accumulation in this short-term experiment, but this effect requires further verification through long-term monitoring.

Competing interest

At least one of the (co-)authors is a member of the editorial board of Biogeosciences.

Author contribution

SV designed the research. AV and JR conducted the experimental work. JR did the data analysis and drafted the paper. All authors contributed to the interpretation of the data and the writing of the manuscript.

References

Aihemaiti, A., Gao, Y., Meng, Y., Chen, X., Liu, J., Xiang, H., Xu, Y., & Jiang, J. (2020). Review of plant-vanadium physiological interactions , bioaccumulation , and bioremediation of vanadium-contaminated sites. *Science of the Total Environment*, *712*, 135637. https://doi.org/10.1016/j.scitotenv.2019.135637

Amann, T., Hartmann, J., Struyf, E., De Oliveira Garcia, W., Fischer, E. K., Janssens, I., Meire, P., & Schoelynck, J. (2020). Enhanced Weathering and related element fluxes - A cropland mesocosm approach. *Biogeosciences*, *17*, 103–119. https://doi.org/10.5194/bg-17-103-2020

Anda, M., Shamshuddin, J., & Fauziah, C. I. (2015). Improving chemical properties of a highly weathered soil using finely ground basalt rocks. *Catena*, *124*, 147–161. https://doi.org/10.1016/j.catena.2014.09.012

Beerling, D. J., Kantzas, E. P., Lomas, M. R., Wade, P., Eufrasio, R. M., Renforth, P., Sarkar, B., Andrews, M. G., James, R. H., Pearce, C. R., Mercure, J. F., Pollitt, H., Holden, P. B., Edwards, N. R., Khanna, M., Koh, L., Quegan, S., Pidgeon, N. F., Janssens, I. A., … Banwart, S. A. (2020). Potential for large-scale CO2 removal via enhanced rock weathering with croplands. *Nature*, *583*, 242–248. https://doi.org/10.1038/s41586-020-2448-9

Berner, R. A. (2004). *The Phanerozoic Carbon Cycle: CO2 and O2*. Oxford University Press. https://doi.org/10.1093/oso/9780195173338.001.0001

Berner, R. A., Lasaga, A. C., & Garrels, R. M. (1983). The carbonate-silicate geochemical cycle and its effect on atmospheric carbon dioxide over the past 100 million years. *American Journal of Science*, *283*, 641–683.

Bhatt, D., & Sharma, G. (2018). Role of silicon in counteracting abiotic and biotic plant stresses. *International Journal of Chemical Studies*, *6*, 1434–1442.

Boniao, R. D., Shamshuddin, J., Van Ranst, E., Zauyah, S., & Syed Omar, S. R. (2002). Changes in chemical properties and growth of corn in volcanic soils treated with peat, ground basalt pyroclastics, and calcium silicate. *Communications in Soil Science and Plant Analysis*, *33*(7–8), 1219–1233. https://doi.org/10.1081/CSS-120003883

Branca, T. A., Pistocchi, C., Colla, V., Ragaglini, G., Amato, A., Tozzini, C., Mudersbach, D., Morillon, A., Rex, M., & Romaniello, L. (2014). *Investigation of \(BOF\) Converter slag use for agriculture in europe*. *167*, 155–167. https://doi.org/10.1051/metal/2014022

Brown, I. C. (1943). A rapid method of determining exchangeable hydrogen and total exchangeable bases of soils. *Soil Science*, *56*, 353–357.

Buckingham, F. L., & Henderson, G. M. (2024). The enhanced weathering potential of a range of silicate and carbonate additions in a UK agricultural soil. *Science of the Total Environment*, *907*, 167701. https://doi.org/10.1016/j.scitotenv.2023.167701

Calabrese, S., Wild, B., Bertagni, M. B., Bourg, I. C., White, C., Aburto, F., Cipolla, G., Noto, L. V., & Porporato, A. (2022). Nano- to Global-Scale Uncertainties in Terrestrial Enhanced Weathering. *Environmental Science and Technology*, *56*, 15261–15272. https://doi.org/10.1021/acs.est.2c03163

Castro, G. S. A., & Crusciol, C. A. C. (2013). Yield and mineral nutrition of soybean, maize, and congo signal grass as affected by limestone and slag. *Pesquisa Agropecuaria Brasileira*, *48*(6), 673–681. https://doi.org/10.1590/S0100-204X2013000600013

Chen, L., Liu, J., Hu, W., Gao, J., & Yang, J. (2021). Vanadium in soil-plant system : Source , fate , toxicity , and bioremediation. *Journal of Hazardous Materials*, *405*, 124200. https://doi.org/10.1016/j.jhazmat.2020.124200

Conceição, L. T., Silva, G. N., Holsback, H. M. S., Oliveira, C. de F., Marcante, N. C., Martins, É. de S., Santos, F. L. de S., & Santos, E. F. (2022). Potential of basalt dust to improve soil fertility and crop nutrition. *Journal of Agriculture and Food Research*, *10*, 100443. https://doi.org/10.1016/j.jafr.2022.100443

De Windt, L., Chaurand, P., & Rose, J. (2011). Kinetics of steel slag leaching: Batch tests and modeling. *Waste Management*, *31*(2), 225–235. https://doi.org/10.1016/j.wasman.2010.05.018

Deus, A. C. F., Büll, L. T., Guppy, C. N., Santos, S. de M. C., & Moreira, L. L. Q. (2020). Effects of lime and steel slag application on soil fertility and soybean yield under a no till-system. *Soil and Tillage Research*, *196*, 104422. https://doi.org/10.1016/j.still.2019.104422

Dieleman, W. I. J., & Janssens, I. A. (2011). Can publication bias affect ecological research ? A case study on soil respiration under elevated CO2. *New Phytologist*, 517–521.

dos Reis, G. S., Thue, P. S., Cazacliu, B. G., Lima, E. C., Sampaio, C. H., Quattrone, M., Ovsyannikova, E., Kruse, A., & Dotto, G. L. (2020). Effect of concrete carbonation on phosphate removal through adsorption process and its potential application as fertilizer. *Journal of Cleaner Production*, *256*. https://doi.org/10.1016/j.jclepro.2020.120416

Dupla, X., Möller, B., Baveye, P. C., & Grand, S. (2023). Potential accumulation of toxic trace elements in soils during enhanced rock weathering. *European Journal of Soil Science*, *74*(1). https://doi.org/10.1111/ejss.13343

Edwards, D. P., Lim, F., James, R. H., Pearce, C. R., Scholes, J., Freckleton, R. P., Beerling, D. J., & Edwards, D. P. (2017). Climate change mitigation: potential benefits and pitfalls of enhanced rock weathering in tropical agriculture. *Biology Letters*, *13*, 20160715.

Ertani, A., Mietto, A., & Borin, M. (2017). Chromium in Agricultural Soils and Crops : A Review. *Water, Air & Soil Pollution*, *228*, 190. https://doi.org/10.1007/s11270-017-3356-y

Fu, S., & Cheng, W. (2002). Rhizosphere priming effects on the decomposition of soil organic matter in C 4 and C 3 grassland soils. *Plant and Soil*, *238*, 289–294.

Gao, D., Wang, F. P., Wang, Y. T., & Zeng, Y. N. (2020). Sustainable utilization of steel slag from traditional industry and agriculture to catalysis. *Sustainability (Switzerland)*, *12*(21), 1–9. https://doi.org/10.3390/su12219295

Gillman, G. P., Burkett, D. C., & Coventry, R. J. (2001). A laboratory study of application of basalt dust to highly weathered soils: Effect on soil cation chemistry. *Australian Journal of Soil Research*, *39*(4), 799–811. https://doi.org/10.1071/SR00073

Goll, D. S., Ciais, P., Amann, T., Buermann, W., Chang, J., Eker, S., Hartmann, J., Janssens, I., Li, W., & Obersteiner, M. (2021). Potential CO2 removal from enhanced weathering by ecosystem responses to powdered rock. *Nature Geoscience*, *14*, 545–549. https://doi.org/10.1038/s41561-021-00798-x

Gudbrandsson, S., Wolff-Boenisch, D., Gislason, S. R., & Oelkers, E. H. (2011). An experimental study of crystalline basalt dissolution from 2pH11 and temperatures from 5 to 75°C. *Geochimica et Cosmochimica Acta*, *75*(19), 5496–5509. https://doi.org/10.1016/j.gca.2011.06.035

Guo, F., Wang, Y., Zhu, H., Zhang, C., Sun, H., Fang, Z., Yang, J., Zhang, L., Mu, Y., Man, Y. B., & Wu, F. (2023). Crop productivity and soil inorganic carbon change mediated by enhanced rock weathering in farmland: A comparative field analysis of multi-agroclimatic regions in central China. *Agricultural Systems*, *210*. https://doi.org/10.1016/j.agsy.2023.103691

Guo, W., Nazim, H., Liang, Z., & Yang, D. (2016). Magnesium deficiency in plants: An urgent problem. *Crop Journal*, *4*(2), 83–91. https://doi.org/10.1016/j.cj.2015.11.003

Haque, F., Santos, R. M., Dutta, A., Thimmanagari, M., & Chiang, Y. W. (2019). Co-Benefits of Wollastonite Weathering in Agriculture: CO2 Sequestration and Promoted Plant Growth. *ACS Omega*, *4*(1), 1425–1433. https://doi.org/10.1021/acsomega.8b02477

Hawkesford, M., Horst, W., Kichey, T., Lambers, H., Schjoerring, J., Skrumsager, I., & White, P. (2012). Functions of Macronutrients. In *Marschner''s Mineral Nutrition of Higher Plants*. Elsevier Ltd. https://doi.org/10.1016/B978-0-12-384905-2.00006-6

He, H., Xiao, Q., Yuan, M., Huang, R., Sun, X., Wang, X., & Zhao, H. (2020). Effects of steel slag amendments on accumulation of cadmium and arsenic by rice (Oryza sativa) in a historically contaminated paddy field. *Environmental Science and Pollution Research*, *27*, 40001–40008. https://doi.org/10.1007/s11356-020-10028-3

Hochmuth, G. J., Maynard, D., Vavrina, C., Hanlon, E., & Simonne, E. (2012). Plant Tissue Analysis and Interpretation for Vegetable Crops in Florida: HS964/EP081 rev. 10/2012. *Edis*, *10*. https://doi.org/10.32473/edis-ep081-2004

Hope, R. M. (2023). *Rmisc: Ryan Miscellaneous. R package version 1.5.1*. https://cran.r-project.org/web/packages/Rmisc

Kassambara, A. (2023). ggpubr: "ggplot2" Based Publication Ready Plots. *R Package Version 0.6.0*. https://rpkgs.datanovia.com/ggpubr/

Kelland, M. E., Wade, P. W., Lewis, A. L., Taylor, L. L., Sarkar, B., Andrews, M. G., Lomas, M. R., Cotton, T. E. A., Kemp, S. J., James, R. H., Pearce, C. R., Hartley, S. E., Hodson, M. E., Leake, J. R., Banwart, S. A., & Beerling, D. J. (2020). Increased yield and CO2 sequestration potential with the C4 cereal Sorghum bicolor cultivated in basaltic rock dust-amended agricultural soil. *Global Change Biology*, *26*(6), 3658–3676. https://doi.org/10.1111/gcb.15089

Kicińska, A., Pomykała, R., & Izquierdo-Diaz, M. (2022). Changes in soil pH and mobility of heavy metals in contaminated soils. *European Journal of Soil Science*, *73*(1). https://doi.org/10.1111/ejss.13203

Klitzke, S., & Lang, F. (2009). Mobilization of Soluble and Dispersible Lead, Arsenic, and Antimony in a Polluted, Organic-rich Soil – Eff ects of pH Increase and Counterion Valency. *Environmental Qualiry*, *38*, 933–939. https://doi.org/10.2134/jeq2008.0239

Kögel-Knabner, I., Wiesmeier, M., & Mayer, S. (2022). *Mechanisms of soil organic carbon sequestration and implications for management* (pp. 11–46). https://doi.org/10.19103/as.2022.0106.02

Kopsell, D. E., Kopsell, D. A., Sams, C. E., & Casey, T. (2013). Ratio of Calcium to Magnesum influences biomass, elemental accumulations, and pigment concentrations in kale. *Journal of Plant Nutrition*, *36*, 2154–2165. https://doi.org/10.1080/01904167.2013.789108

Kushwaha, A., Hans, N., Kumar, S., & Rani, R. (2018). A critical review on speciation, mobilization and toxicity of lead in soil-microbe-plant system and bioremediation strategies. *Ecotoxicology and Environmental Safety*, *147*, 1035–1045. https://doi.org/10.1016/j.ecoenv.2017.09.049

Kuzyakov, Y. (2002). Review: Factors affecting rhizosphere priming effects. *Journal of Plant Nutrition and Soil Science*, *165*, 382–396.

Lehmann, N., Lantuit, H., Böttcher, M. E., Hartmann, J., Eulenburg, A., & Thomas, H. (2023). Alkalinity generation from carbonate weathering in a silicate-dominated headwater catchment at Iskorasfjellet, northern Norway. *Biogeosciences*, *20*(16), 3459–3479. https://doi.org/10.5194/bg-20-3459-2023

Lewis, A. L., Sarkar, B., Wade, P., Kemp, S. J., Hodson, M. E., Taylor, L. L., Yeong, K. L., Davies, K., Nelson, P. N., Bird, M. I., Kantola, I. B., Masters, M. D., DeLucia, E., Leake, J. R., Banwart, S. A., & Beerling, D. J. (2021). Effects of mineralogy, chemistry and physical properties of basalts on carbon capture potential and plant-nutrient element release via enhanced weathering. *Applied Geochemistry*, *132*(June), 105023. https://doi.org/10.1016/j.apgeochem.2021.105023

Li, L., Scheckel, K. G., Zheng, L., Liu, G., Xing, W., & Xiang, G. (2014). Immobilization of Lead in Soil Influenced by Soluble Phosphate and Calcium: Lead Speciation Evidence. *Journal of Environmental Quality*, *43*(2), 468–474. https://doi.org/10.2134/jeq2013.07.0272

Li, P., Karunanidhi, D., Subramani, T., & Srinivasamoorthy, K. (2021). Sources and Consequences of Groundwater Contamination. In *Archives of Environmental Contamination and Toxicology* (Vol. 80, Issue 1). Springer. https://doi.org/10.1007/s00244-020-00805-z

Lindsay, W. L., Schwab, A. P., State, C., & Collins, F. (2008). The chemistry of iron in soils and its availability to plants. *Journal of Plant Nutrition*, *5*, 821–840.

Liu, Z., Dreybrodt, W., & Liu, H. (2011). Atmospheric CO2 sink: Silicate weathering or carbonate weathering? *Applied Geochemistry*, *26*(SUPPL.). https://doi.org/10.1016/j.apgeochem.2011.03.085

Lizárraga-paulín, E. G., Torres-pacheco, I., Moreno-martínez, E., & Miranda-castro, S. P. (2011). Chitosan application in maize (Zea mays) to counteract the effects of abiotic stress at seedling level. *African Journal of Biotechnology*, *10*, 6439–6446. https://doi.org/10.5897/AJB10.1448

Luchese, A. V., Gutz de Castro Leite, I. J., da Silva Giaretta, A. P., Alves, M. L., Pivetta, L. A., & Missio, R. F. (2023). Use of quarry waste basalt rock powder as a soil remineralizer to grow soybean and maize. *Heliyon*, *9*, e14050. https://doi.org/10.1016/j.heliyon.2023.e14050

Majeed, S., Reetika, Z., Javaid, M., Muslima, A. B., & Rupesh, N. (2019). Role of silicon in plant stress tolerance : opportunities to achieve a sustainable cropping system. *3 Biotech*, *9*, 1–16. https://doi.org/10.1007/s13205-019-1613-z

Makabe-sasaki, S., & Sasaki, Y. (2015). *Effects of slag silicate fertilizer on silicon content of rice plants grown in paddy fields on the Shounai Plain , Yamagata , Japan*. *September 2014*. https://doi.org/10.1080/00380768.2014.936305

Montgomery, E. G. (1911). Correlation studies in corn. *Neb. Agric. Exp. Stn. Annu. Rep*, *24*, 108–159.

Moosdorf, N., Renforth, P., & Hartmann, J. (2014). *Carbon Dioxide E ffi ciency of Terrestrial Enhanced Weathering*.

Nagajyoti, P. C., Lee, K. D., & Sreekanth, T. V. M. (2010). Heavy metals, occurrence and toxicity for plants: A review. *Environmental Chemistry Letters*, *8*, 199–216. https://doi.org/10.1007/s10311-010-0297-8

Ning, D., Song, A., Fan, F., Li, Z., & Liang, Y. (2014). Effects of Slag-Based Silicon Fertilizer on Rice Growth and Brown-Spot Resistance. *PLoS ONE*, *9*, 1–9. https://doi.org/10.1371/journal.pone.0102681

O'Connor, J., Nguyen, T. B. T., Honeyands, T., Monaghan, B., O'Dea, D., Rinklebe, J., Vinu, A., Hoang, S. A., Singh, G., Kirkham, M. B., & Bolan, N. (2021). Production, characterisation, utilisation, and beneficial soil application of steel slag: A review. *Journal of Hazardous Materials*, *419*(May). https://doi.org/10.1016/j.jhazmat.2021.126478

Osemwota, I. O. (2007). Effect of Calcium / Magnesium Ratio in Soil on Magnesium Availability , Yield , and Yield Components of Maize. *Communications in Soil Science and Plant Analysis*, *38*, 2849–2860. https://doi.org/10.1080/00103620701663081

Palandri, J., & Kharaka, Y. (2004). A compilation of rate parameters of water-mineral interaction kinerics for application to geochemical modeling. In *U.S. Geologival Survey*.

Pinheiro, J., Bates, D., Debroy, S., Sarka, D., & R Core Team, R. (2013). nlme: Linear and Nonlinear Mixed Effects Models. *R Package Version 3.1*, 109.

Pistocchi, C., Ragaglini, G., Colla, V., Branca, T. A., Tozzini, C., & Romaniello, L. (2017). Exchangeable Sodium Percentage decrease in saline sodic soil after Basic Oxygen Furnace Slag application in a lysimeter trial. *Journal of Environmental Management*, *203*, 896–906. https://doi.org/10.1016/j.jenvman.2017.05.007

Qian, P., & Schoenau, J. J. (2002). Practical applications of ion exchange resins in agricultural and environmental soil research. *Canadian Journal of Soil Science*, *82*, 9–21.

Ramezanian, A., Dahlin, A. S., Campbell, C. D., Hillier, S., Mannerstedt-Fogelfors, B., & Öborn, I. (2013). Addition of a volcanic rockdust to soils has no observable effects on plant yield and nutrient status or on soil microbial activity. *Plant and Soil*, *367*, 419–436. https://doi.org/10.1007/s11104-012-1474-2

Ramos, C. G., Hower, J. C., Blanco, E., Oliveira, M. L. S., & Theodoro, S. H. (2022). Possibilities of using silicate rock powder: An overview. *Geoscience Frontiers*, *13*(1), 101185. https://doi.org/10.1016/j.gsf.2021.101185

Renforth, P., Washbourne, C. L., Taylder, J., & Manning, D. A. C. (2011). Silicate production and availability for mineral carbonation. *Environmental Science and Technology*, *45*, 2035–2041. https://doi.org/10.1021/es103241w

Rijnders, J., Vicca, S., Struyf, E., Amann, T., Hartmann, J., Meire, P., Janssens, I., & Schoelynck, J. (2023). The effects of dunite fertilization on growth and elemental composition of barley and wheat differ with dunite grain size and rainfall regimes. *Frontiers in Environmental Science*, *11*(August), 1–18. https://doi.org/10.3389/fenvs.2023.1172621

Roychoudhury, A. (2020). Vanadium Uptake and Toxicity in Plants. *SF Journal of Agricultural and Crop Management*, *12*, 1010.

Sbai, K., Tahri, L., Hafiane, F. Z., Halima, O. I., & Fekhaoui, M. (2024). Assessment of heavy metal pollution in groundwater using a multivariate analysis approach. *Journal of Water and Land Development*, *61*, 175–182. https://doi.org/10.24425/jwld.2024.150272

Schlüter, U., Mascher, M., Colmsee, C., Scholz, U., Bräutigam, A., Fahnenstich, H., & Sonnewald, U. (2012). Maize source leaf adaptation to nitrogen deficiency affects not only nitrogen and carbon metabolism but also control of phosphate homeostasis. *Plant Physiology*, *160*, 1384–1406. https://doi.org/10.1104/pp.112.204420

Shenker, M., & Chen, Y. (2005). Increasing Iron Availability to Crops: Fertilizers, Organo-Fertilizers, and Biological Approaches. *Soil Science and Plant Nutrition*, *51*, 1–17.

Skov, K., Wardman, J., Healey, M., Mcbride, A., Bierowiec, T., Cooper, J., Edeh, I., George, D., Kelland, M. E., Mann, J., Manning, D., Murphy, M. J., Pape, R., Teh, Y. A., Id, W. T., Wade, P., & Liu, X. (2024). Initial agronomic benefits of enhanced weathering using basalt : A study of spring oat in a temperate climate. *PLoS ONE*, *19*, 1–20. https://doi.org/10.1371/journal.pone.0295031

Sreekanth, T. V. M., Nagajyothi, P. C., Lee, K. D., & Prasad, T. N. V. K. V. (2013). Occurrence , physiological responses and toxicity of nickel in plants. *International Journal of Environmental Science and Technology*, *10*, 1129–1140. https://doi.org/10.1007/s13762-013-0245-9

Swoboda, P., Döring, T. F., & Hamer, M. (2022). Remineralizing soils? The agricultural usage of silicate rock powders: A review. In *Science of the Total Environment* (Vol. 807). Elsevier B.V. https://doi.org/10.1016/j.scitotenv.2021.150976

Taylor, L. L., Beerling, D. J., Quegan, S., & Banwart, S. A. (2017). Simulating carbon capture by enhanced weathering with croplands: An overview of key processes highlighting areas of future model development. *Biology Letters*, *13*(4). https://doi.org/10.1098/rsbl.2016.0868

Tchouankoue, J. P. (2014). Soil Remineralization Trial: Preliminary Effects of Montserrat Volcanic Ash on Barbuda Limestone soils. *Geotherapy*, *October*, 391–398. https://doi.org/10.1201/b13788-27

Ten Berge, H. F. M., Meer, H. G. Van Der, Steenhuizen, J. W., Goedhart, P. W., Knops, P., & Verhagen, J. (2012). Olivine Weathering in Soil , and Its Effects on Growth and Nutrient Uptake in Ryegrass (Lolium perenne L .): A Pot Experiment. *PLoS ONE*, *7*, 42098. https://doi.org/10.1371/journal.pone.0042098

Tilman, D., Cassman, K. G., Matson, P. A., Naylor, R., & Polasky, S. (2002). Agricultural sustainability and intensive production practices. *Nature*, *418*, 671–677. www.nature.com/nature

Van Straaten, P. (2006). Farming with rocks and minerals: Challenges and opportunities. *Anais Da Academia Brasileira de Ciencias*, *78*, 731–747. https://doi.org/10.1590/S0001-37652006000400009

Ven, A., Verlinden, M. S., Fransen, E., Olsson, P. A., Verbruggen, E., Wallander, H., & Vicca, S. (2020). Phosphorus addition increased carbon partitioning to autotrophic respiration but not to biomass production in an experiment with Zea mays. *Plant Cell and Environment*, *43*(9), 2054–2065. https://doi.org/10.1111/pce.13785

Ven, A., Verlinden, M. S., Verbruggen, E., & Vicca, S. (2019). Experimental evidence that phosphorus fertilization and arbuscular mycorrhizal symbiosis can reduce the carbon cost of phosphorus uptake. *Functional Ecology*, *33*(11), 2215–2225. https://doi.org/10.1111/1365-2435.13452

Vienne, A., Poblador, S., Portillo-estrada, M., & Hartmann, J. (2022). Enhanced Weathering Using Basalt Rock Powder : Carbon Sequestration , Co-benefits and Risks in a Mesocosm Study With Solanum tuberosum. *Frontiers in Climate*, *May*, 869456. https://doi.org/10.3389/fclim.2022.869456

Walinga, I., Van Der Lee, J. J., Houba, V. J. G., Van Vark, W., & Novozamsky, I. (1995). Plant Analysis Manual. In *Plant Analysis Manual*. Springer Netherlands. https://doi.org/10.1007/978-94-011-0203-2

Walker, J. C. G., Hays, P. B., & Kasting, J. F. (1981). A negative feedback mechanism for the long-term stabilization of Earth’s surface temperature. *Journal of Geophysical Research*, *86*(C10), 9776–9782. https://doi.org/10.1029/JC086iC10p09776

Wang, W., Sardans, J., Lai, D. Y. F., Wang, C., Zeng, C., Tong, C., & Liang, Y. (2015). Field Crops Research Effects of steel slag application on greenhouse gas emissions and crop yield over multiple growing seasons in a subtropical paddy field in China. *Field Crops Research*, *171*, 146–156. https://doi.org/10.1016/j.fcr.2014.10.014

Wang, X., & Qing-sheng, C. (2006). Steel Slag as an Iron Fertilizer for Corn Growth and Soil Improvement in a Pot Experiment *’. *Soil Science Society of China*, *16*, 519–524.

White, A. F., Schulz, M. S., Lawrence, C. R., Vivit, D. V., & Stonestrom, D. A. (2017). Long-term flow-through column experiments and their relevance to natural granitoid weathering rates. *Geochimica et Cosmochimica Acta*, *202*, 190–214. https://doi.org/10.1016/j.gca.2016.11.042

WHO, & FAO. (2022). *General standards for contaminants and toxins in food and feed*.

Wickham, H. (2016). Data Analysis. In *ggplot2: Elegant Graphics for Data Analysis* (pp. 189–201). Springer International Publishing. https://doi.org/10.1007/978-3-319-24277-4_9

Yan, Y., Dong, X., Li, R., Zhang, Y., Yan, S., Guan, X., Yang, Q., Chen, L., Fang, Y., Zhang, W., & Wang, S. (2023). Wollastonite addition stimulates soil organic carbon mineralization: Evidences from 12 land-use types in subtropical China. *Catena*, *225*(November 2022), 107031. https://doi.org/10.1016/j.catena.2023.107031

Yusuf, M., Fariduddin, Q., Hayat, S., & Ahmad, A. (2011). Nickel: An overview of uptake, essentiality and toxicity in plants. *Bulletin of Environmental Contamination and Toxicology*, *86*, 1–17. https://doi.org/10.1007/s00128-010-0171-1